

$B \rightarrow \rho(\omega, \phi)\eta^{(\prime)}$ Decays and NLO contributions in the pQCD Approach

Zhi-Qing Zhang^a and Zhen-jun Xiao^{a,b *}

*a. Department of Physics and Institute of Theoretical Physics,
Nanjing Normal University, Nanjing, Jiangsu 210097, P.R.China and*

b. Kavli Institute for Theoretical Physics China, CAS, Beijing, 100190, China

(Dated: October 30, 2018)

Abstract

By employing the perturbative QCD (pQCD) factorization approach, we calculated some important next-to-leading-order(NLO) contributions to the two-body charmless hadronic decays $B^+ \rightarrow \rho^+\eta^{(\prime)}$ and $B^0 \rightarrow \rho^0(\omega, \phi)\eta^{(\prime)}$, induced by the vertex QCD corrections, the quark-loops as well as the chromo-magnetic penguins. From the numerical results and phenomenological analysis we find that (a) for $B^\pm \rightarrow \rho^\pm\eta^{(\prime)}$ decays, the partial NLO contributions to branching ratios are small in magnitude; (b) for $B^0 \rightarrow \rho^0(\omega, \phi)\eta^{(\prime)}$ decays, the NLO contributions can provide significant enhancements to the leading order predictions of their branching ratios; and (c) the pQCD predictions for the CP-violating asymmetries $\mathcal{A}_{CP}^{dir}(B^\pm \rightarrow \rho^\pm\eta^{(\prime)})$ are consistent with the data, while the predicted $\mathcal{A}_{CP}(B^0 \rightarrow \rho^0(\omega)\eta^{(\prime)})$ are generally large in magnitude and could be tested by the forthcoming LHCb experiments.

PACS numbers: 13.25.Hw, 12.38.Bx, 14.40.Nd

* Electronic address: xiaozhenjun@njnu.edu.cn

I. INTRODUCTION

During the past decade, the B factory experiments have achieved great successes. More than one billion events of $B\bar{B}$ production and decays have been accumulated and analyzed by BaBar and Belle Collaborations. The forthcoming LHC experiments will provide 2-3 orders more B meson events than the B factory, and high precision measurements for the branching ratios and CP-violating asymmetries of many B meson rare decays will become true within the following three to five years. Now it becomes a very important and urgent task to reduce the uncertainty of the theoretical predictions, in order to test the standard mode (SM) and to find signals or evidence of the new physics beyond the SM through the B meson experiments [1].

For the charmless decays $B \rightarrow M_1 M_2$ (here M_i are light mesons composed of the light u, d, s quarks), the dominant theoretical error comes from the large uncertainty in evaluating the hadronic matrix elements $\langle M_1 M_2 | O_i | B \rangle$. In order to increase the accuracy of the SM predictions, various factorization approaches have been proposed in recent years. The perturbative QCD (pQCD) factorization approach [2] , together with the so-called QCD Factorization (QCDF) [3] and the SCET [4] , are the most popular factorization approaches [3, 4] being used currently to calculate the hadronic matrix elements [3, 5, 6, 7, 8, 9, 10, 11, 12, 13, 14].

When compared with the QCDF or SCET factorization approaches, the pQCD approach has the following three special features: (a) since the k_T factorization is employed here, the resultant Sudakov factor as well as the threshold resummation can enable us to regulate the end-point singularities effectively; (b) the form factors for $B \rightarrow M$ transition can be calculated perturbatively, although some controversies still exist about this point; and (c) the annihilation diagrams are calculable and play an important role in producing CP violation.

Up to now, almost all two-body charmless $B/B_s \rightarrow M_1 M_2$ decays have been calculated by using the pQCD approach at the leading order (LO) [6, 7, 8, 9, 10, 11, 12, 13, 14]. Very recently, some next-to-leading (NLO) contributions to $B \rightarrow K\pi$ and several $B \rightarrow PV$ decay modes [15, 16] have been calculated, where the Wilson coefficients at NLO accuracy are used, and the contributions from the vertex corrections, the quark loops and the chromo-magnetic penguin operator O_{8g} have been taken into account. As generally expected, the inclusion of NLO contributions should improve the reliability of the pQCD predictions.

In previous papers [10, 11], the authors calculated the branching ratios and CP violating asymmetries of the $B \rightarrow \rho(\omega, \phi)\eta^{(\prime)}$ decays by employing the pQCD approach at the leading order. Following the procedure of Ref. [15], we here would like to calculate the NLO contributions to the $B \rightarrow \rho(\omega, \phi)\eta^{(\prime)}$ decays by employing the low energy effective Hamiltonian and the pQCD approach.

The remainder of the paper is organized as follows. In Sec.II, we give a brief discussion about pQCD factorization approach. In Sec. III, we calculate analytically the relevant Feynman diagrams and present the various decay amplitudes for the studied decay modes in leading-order. In Sec. IV, the NLO contributions from the vertex corrections, the quark loops and the chromo-magnetic penguin amplitudes are evaluated. We show the numerical results for the branching ratios and CP asymmetries of $B \rightarrow \rho(\omega, \phi)\eta^{(\prime)}$ decays in Sec. V. The summary and some discussions are included in the final section.

II. THEORETICAL FRAMEWORK

Based on the pQCD factorization approach [2], the decay amplitude $\mathcal{A}(B \rightarrow M_1 M_2)$ can be written conceptually as the convolution,

$$\mathcal{A}(B \rightarrow M_1 M_2) \sim \int d^4 k_1 d^4 k_2 d^4 k_3 \text{Tr} [C(t) \Phi_B(k_1) \Phi_{M_1}(k_2) \Phi_{M_2}(k_3) H(k_1, k_2, k_3, t)], \quad (1)$$

where k_i 's are momenta of light quarks included in each meson, and Tr denotes the trace over Dirac and color indices. $C(t)$ is the Wilson coefficient evaluated at scale t . The function $H(k_1, k_2, k_3, t)$ describes the four quark operator and the spectator quark connected by a hard gluon and could be calculated perturbatively. The function Φ_B and Φ_{M_i} are the wave functions of the initial heavy B meson and the final light meson M_i , which describe the hadronization of the quark and anti-quark into the mesons. While the hard kernel H depends on the processes considered, the wave functions Φ_B and Φ_{M_i} are independent of the specific processes.

In the B meson rest-frame, it is convenient to use light-cone coordinate (p^+, p^-, \mathbf{p}_T) to describe the meson's momenta: $p^\pm = \frac{1}{\sqrt{2}}(p^0 \pm p^3)$ and $\mathbf{p}_T = (p^1, p^2)$. Using these coordinates the B meson and the two final state meson momenta can be written as

$$P_B = \frac{M_B}{\sqrt{2}}(1, 1, \mathbf{0}_T), \quad P_V = \frac{M_B}{\sqrt{2}}(1, r_V^2, \mathbf{0}_T), \quad P_P = \frac{M_B}{\sqrt{2}}(0, 1 - r_V^2, \mathbf{0}_T), \quad (2)$$

respectively, here $r_V = m_V/M_B$ with $V = \rho, \omega$ or ϕ . The light meson ($P = \eta^{(\prime)}$) mass has been neglected. For the $B \rightarrow VP$ decays considered here, only the vector meson's longitudinal part contributes to the decays, and its polarization vector is $\epsilon_L = \frac{M_B}{\sqrt{2}M_V}(1, -r_V^2, \mathbf{0}_T)$. Putting the anti-quark momenta in B , V and P mesons as k_1 , k_2 , and k_3 , respectively, we can choose

$$k_1 = (x_1 P_1^+, 0, \mathbf{k}_{1T}), \quad k_2 = (x_2 P_2^+, 0, \mathbf{k}_{2T}), \quad k_3 = (0, x_3 P_3^-, \mathbf{k}_{3T}). \quad (3)$$

Then, the integration over k_1^- , k_2^- , and k_3^+ in eq.(1) will lead to

$$\mathcal{A}(B \rightarrow PV) \sim \int dx_1 dx_2 dx_3 b_1 db_1 b_2 db_2 b_3 db_3 \cdot \text{Tr} [C(t) \Phi_B(x_1, b_1) \Phi_V(x_2, b_2) \Phi_P(x_3, b_3) H(x_i, b_i, t) S_t(x_i) e^{-S(t)}], \quad (4)$$

where b_i is the conjugate space coordinate of k_{iT} . The large logarithms ($\ln m_W/t$) coming from QCD radiative corrections to four quark operators are included in the Wilson coefficients $C(t)$. The large double logarithms ($\ln^2 x_i$) on the longitudinal direction are summed by the threshold resummation [17], and they lead to $S_t(x_i)$ which smears the end-point singularities on x_i . The last term, $e^{-S(t)}$, is the Sudakov form factor which suppresses the soft dynamics effectively [2].

For the studied $B \rightarrow V\eta^{(\prime)}$ decays, the weak effective Hamiltonian H_{eff} can be written as [18]

$$\mathcal{H}_{eff} = \frac{G_F}{\sqrt{2}} \sum_{q=u,c} V_{qb} V_{qd}^* \left[(C_1(\mu) O_1^q(\mu) + C_2(\mu) O_2^q(\mu)) + \sum_{i=3}^{10} C_i(\mu) O_i(\mu) \right]. \quad (5)$$

where $G_F = 1.16639 \times 10^{-5} GeV^{-2}$ is the Fermi constant, and V_{ij} is the CKM matrix element, $C_i(\mu)$ are the Wilson coefficients evaluated at the renormalization scale μ and $O_i(\mu)$ are the four-fermion operators. For the case of $b \rightarrow s$ transition, simply make a replacement of d by s in Eq. (5) and in the expressions of $O_i(\mu)$ operators, which can be found easily for example in Refs.[12, 18].

In PQCD approach, the energy scale “ t ” is chosen as the largest energy scale in the hard kernel $H(x_i, b_i, t)$ of a given Feynman diagram, in order to suppress the higher order corrections and improve the reliability of the perturbative calculation. Here, the scale “ t ” may be larger or smaller than the m_b scale. In the range of $t < m_b$ or $t \geq m_b$, the number of active quarks is $N_f = 4$ or $N_f = 5$, respectively. For the Wilson coefficients $C_i(\mu)$ and their renormalization group (RG) running, they are known at NLO level currently [18]. The explicit expressions of the LO and NLO $C_i(m_W)$ can be found easily, for example, in Refs. [7, 18].

When the pQCD approach at leading-order are employed, the leading order Wilson coefficients $C_i(m_W)$, the leading order RG evolution matrix $U(t, m)^{(0)}$ from the high scale m down to $t < m$ (for details see Eq. (3.94) in Ref. [18]), and the leading order $\alpha_s(t)$ are used:

$$\alpha_s(t) = \frac{4\pi}{\beta_0 \ln [t^2/\Lambda_{QCD}^2]}, \quad (6)$$

where $\beta_0 = (33 - 2N_f)/3$, $\Lambda_{QCD}^{(5)} = 0.225 GeV$ and $\Lambda_{QCD}^{(4)} = 0.287 GeV$.

When the NLO contributions are taken into account, however, the NLO Wilson coefficients $C_i(m_W)$, the NLO RG evolution matrix $U(t, m, \alpha)$ (for details see Eq. (7.22) in Ref. [18]) and the $\alpha_s(t)$ at two-loop level are used:

$$\alpha_s(t) = \frac{4\pi}{\beta_0 \ln [t^2/\Lambda_{QCD}^2]} \cdot \left\{ 1 - \frac{\beta_1}{\beta_0^2} \cdot \frac{\ln [\ln [t^2/\Lambda_{QCD}^2]]}{\ln [t^2/\Lambda_{QCD}^2]} \right\}, \quad (7)$$

where $\beta_0 = (33 - 2N_f)/3$, $\beta_1 = (306 - 38N_f)/3$, $\Lambda_{QCD}^{(5)} = 0.225 GeV$ and $\Lambda_{QCD}^{(4)} = 0.326 GeV$.

III. DECAY AMPLITUDES AT LEADING ORDER

In the pQCD approach, the Feynman diagrams as shown in Fig. 1 may contribute to $B \rightarrow \rho(\omega, \phi)\eta^{(l)}$ decays at leading order. These decays have been studied previously in Refs. [10, 11] by using the pQCD approach. In this paper, we focus on the calculations of some NLO contributions to these decays in the pQCD approach. We firstly recalculated and confirmed the previous calculation. For the sake of completeness, we present the relevant LO decay amplitudes in this section.

At the leading order, the total decay amplitudes for $B \rightarrow \rho\eta$, $B^0 \rightarrow \omega\eta$, and $B^0 \rightarrow \phi\eta$

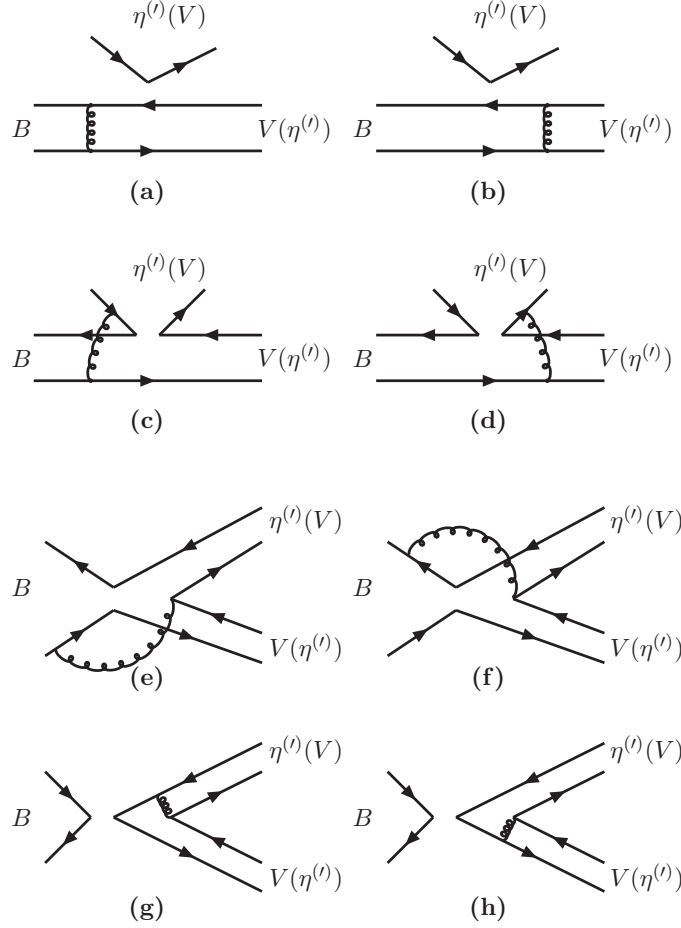


FIG. 1: Feynman diagrams which may contribute to the $B \rightarrow \rho(\omega, \phi)\eta^{(\prime)}$ decays at leading order.

can be written as [10, 11]

$$\begin{aligned}
\mathcal{M}(\rho^+\eta) = & F_{e\rho} \left\{ \left[\xi_u a_2 - \xi_t \left(2a_3 + a_4 - 2a_5 - \frac{1}{2}a_7 + \frac{1}{2}a_9 - \frac{1}{2}a_{10} \right) \right] f_\eta^q \right. \\
& \left. - \xi_t \left(a_3 - \frac{1}{2}a_9 - a_5 + \frac{1}{2}a_7 \right) f_\eta^s \right\} - F_{e\rho}^{P2} \xi_t \left(a_6 - \frac{1}{2}a_8 \right) f_\eta^q \\
& + M_{e\rho} \left\{ \left[\xi_u C_2 - \xi_t \left(C_3 + 2C_4 + 2C_6 + \frac{1}{2}C_8 - \frac{1}{2}C_9 + \frac{1}{2}C_{10} \right) \right] F_1(\phi) \right. \\
& \left. - \xi_t \left(C_4 + C_6 - \frac{1}{2}C_8 - \frac{1}{2}C_{10} \right) F_2(\phi) \right\} \\
& + (M_{a\rho} + M_e + M_a) [\xi_u C_1 - \xi_t (C_3 + C_9)] F_1(\phi) \\
& - (M_{a\rho}^{P1} + M_a^{P1} + M_e^{P1}) (C_5 + C_7) F_1(\phi) \\
& + F_e f_\rho [\xi_u a_1 - \xi_t (a_4 + a_{10})] F_1(\phi),
\end{aligned} \tag{8}$$

$$\begin{aligned}
\sqrt{2}\mathcal{M}(\rho^0\eta) = & -F_{e\rho} \left\{ \left[\xi_u a_2 - \xi_t \left(2a_3 + a_4 - 2a_5 - \frac{1}{2}a_7 + \frac{1}{2}a_9 - \frac{1}{2}a_{10} \right) \right] f_\eta^q \right. \\
& \left. - \xi_t \left(a_3 - \frac{1}{2}a_9 - a_5 + \frac{1}{2}a_7 \right) f_\eta^s \right\} - F_{e\rho}^{P2} \xi_t \left(a_6 - \frac{1}{2}a_8 \right) f_\eta^q \\
& - M_{e\rho} \left\{ \left[\xi_u C_2 - \xi_t \left(C_3 + 2C_4 + 2C_6 + \frac{1}{2}C_8 - \frac{1}{2}C_9 + \frac{1}{2}C_{10} \right) \right] F_1(\phi) \right. \\
& \left. - \xi_t \left(C_4 + C_6 - \frac{1}{2}C_8 - \frac{1}{2}C_{10} \right) F_2(\phi) \right\} \\
& + (M_{a\rho} + M_a) \left[\xi_u C_2 - \xi_t \left(-C_3 + \frac{3}{2}C_8 + \frac{1}{2}C_9 + \frac{3}{2}C_{10} \right) \right] F_1(\phi) \\
& - (M_{a\rho}^{P1} + M_a^{P1} + M_e^{P1}) \xi_t \left(C_5 - \frac{1}{2}C_7 \right) F_1(\phi) \\
& + M_e \left[\xi_u C_2 - \xi_t \left(-C_3 - \frac{3}{2}C_8 + \frac{1}{2}C_9 + \frac{3}{2}C_{10} \right) \right] F_1(\phi) \\
& + F_e f_\rho \left[\xi_u a_1 - \xi_t \left(-a_4 + \frac{3}{2}a_7 + \frac{3}{2}a_9 + \frac{1}{2}a_{10} \right) \right] F_1(\phi), \tag{9}
\end{aligned}$$

$$\begin{aligned}
\sqrt{2}\mathcal{M}(\omega\eta) = & F_{e\omega} \left\{ \left[\xi_u a_2 - \xi_t \left(2a_3 + a_4 - 2a_5 - \frac{1}{2}a_7 + \frac{1}{2}a_9 - \frac{1}{2}a_{10} \right) \right] f_\eta^q \right. \\
& \left. - \xi_t \left(a_3 - \frac{1}{2}a_9 - a_5 + \frac{1}{2}a_7 \right) f_\eta^s \right\} - F_{e\omega}^{P2} \xi_t \left(a_6 - \frac{1}{2}a_8 \right) f_\eta^q \\
& - M_{e\omega} \left\{ \left[\xi_u C_2 - \xi_t \left(C_3 + 2C_4 + 2C_6 + \frac{1}{2}C_8 - \frac{1}{2}C_9 + \frac{1}{2}C_{10} \right) \right] F_1(\phi) \right. \\
& \left. - \xi_t \left(C_4 + C_6 - \frac{1}{2}C_8 - \frac{1}{2}C_{10} \right) F_2(\phi) \right\} \\
& + (M_{a\omega} + M_a) \left[\xi_u C_2 - \xi_t \left(C_3 + 2C_4 - \frac{1}{2}C_9 + \frac{1}{2}C_{10} \right) \right] F_1(\phi) \\
& - (M_{a\omega}^{P1} + M_a^{P1} + M_e^{P1}) \xi_t \left(C_5 - \frac{1}{2}C_7 \right) F_1(\phi) \\
& + M_e \left[\xi_u C_2 - \xi_t \left(C_3 + 2C_4 - 2C_6 - \frac{1}{2}C_8 - \frac{1}{2}C_9 + \frac{1}{2}C_{10} \right) \right] F_1(\phi) \\
& + F_e f_\omega \left[\xi_u a_2 - \xi_t \left(2a_3 + a_4 + 2a_5 + \frac{1}{2}a_7 + \frac{1}{2}a_9 - \frac{1}{2}a_{10} \right) \right] F_1(\phi) \\
& - (M_a^{P2} + M_{a\omega}^{P2}) \xi_t \left(2C_6 + \frac{1}{2}C_8 \right) F_1(\phi), \tag{10}
\end{aligned}$$

$$\begin{aligned}
\mathcal{M}(\phi\eta) = & -F_e f_\phi \xi_t \left(a_3 + a_5 - \frac{1}{2}a_7 - \frac{1}{2}a_9 \right) F_1(\phi) \\
& -M_e \xi_t \left(C_4 - C_6 + \frac{1}{2}C_8 - \frac{1}{2}C_{10} \right) F_1(\phi) \\
& - (M_a + M_{a\phi}) \xi_t \left(C_4 - \frac{1}{2}C_{10} \right) F_2(\phi) \\
& - (M_a^{P2} + M_{a\phi}^{P2}) \xi_t \left(C_6 - \frac{1}{2}C_8 \right) F_2(\phi), \tag{11}
\end{aligned}$$

where $\xi_u = V_{ub}^* V_{ud}$, $\xi_t = V_{tb}^* V_{td}$, and $F_1(\phi), F_2(\phi)$ are the mixing factors of $\eta - \eta'$ system as define in Eq. (A9):

$$F_1(\phi) = \frac{1}{\sqrt{2}} \cos \phi, \quad F_2(\phi) = -\sin \phi. \tag{12}$$

The Wilson coefficients a_i appeared in the expressions of the total decay amplitude are the combinations of the ordinary Wilson coefficients $C_i(\mu)$,

$$\begin{aligned}
a_1(\mu) &= C_2(\mu) + \frac{1}{3}C_1(\mu), \quad a_2(\mu) = C_1(\mu) + \frac{1}{3}C_2(\mu), \\
a_i(\mu) &= C_i(\mu) + \frac{C_{i\pm 1}(\mu)}{3}, \text{ for } i = 3, 5, 7, 9; \text{ or } 4, 6, 8, 10. \tag{13}
\end{aligned}$$

The individual decay amplitudes $F_{e\rho}, \dots$, as given in Eqs. (8-11), are obtained by evaluating individual Feynman diagrams for a given decay mode and can be written as

$$\begin{aligned}
F_{eV} = & 4\sqrt{2}\pi G_F C_F m_B^4 \int_0^1 dx_1 dx_2 \int_0^\infty b_1 db_1 b_2 db_2 \phi_B(x_1, b_1) \\
& \times \left\{ [(1+x_2)\phi_V(\bar{x}_2) - (1-2x_2)r_V(\phi_V^s(\bar{x}_2) - \phi_V^t(\bar{x}_2))] E_e(t_a) h_e(x_1, x_2, b_1, b_2) \right. \\
& \left. - 2r_V \phi_V^s(\bar{x}_2) E_e(t'_a) h_e(x_2, x_1, b_2, b_1) \right\}, \tag{14}
\end{aligned}$$

$$\begin{aligned}
F_{eV}^{P2} = & 8\sqrt{2}G_F \pi C_F m_B^4 \int_0^1 dx_1 dx_2 \int_0^\infty b_1 db_1 b_2 db_2 \phi_B(x_1) \\
& \times \left\{ -r_\eta [\phi_V(\bar{x}_2) - r_V((2+x_2)\phi_V^s(\bar{x}_2) + x_2\phi_V^t(\bar{x}_2))] E_e(t_a) h_e(x_1, x_2, b_1, b_2) \right. \\
& \left. + 2r_V r_\eta \phi_V^s(\bar{x}_2) E_e(t'_a) h_e(x_2, x_1, b_2, b_1) \right\}, \tag{15}
\end{aligned}$$

$$\begin{aligned}
M_{eV} = & M_{eV}^{P2} = \frac{16}{\sqrt{3}} G_F \pi C_F m_B^4 \int_0^1 dx_1 dx_2 dx_3 \int_0^\infty b_1 db_1 b_3 db_3 \phi_B(x_1, b_1) \phi_\eta^A(\bar{x}_3) \\
& \times \left\{ [-x_2 \phi_V(\bar{x}_2) + 2x_2 r_V \phi_V^t(\bar{x}_2)] E'_e(t_b) h_n(x_1, x_2, x_3, b_1, b_3) \right\}, \tag{16}
\end{aligned}$$

$$\begin{aligned}
M_{aV} = & \frac{16}{\sqrt{3}} G_F \pi C_F m_B^4 \int_0^1 dx_1 dx_2 dx_3 \int_0^\infty b_1 db_1 b_3 db_3 \phi_B(x_1, b_1) \\
& \times \left\{ [(1-x_2)\phi_V(\bar{x}_2)\phi_\eta^A(\bar{x}_3) + r_V r_\eta (1-x_2) (\phi_V^s(\bar{x}_2) + \phi_V^t(\bar{x}_2)) (\phi_\eta^P(\bar{x}_3) - \phi_\eta^T(\bar{x}_3)) \right. \\
& \left. + r_V r_\eta x_3 (\phi_V^s(\bar{x}_2) - \phi_V^t(\bar{x}_2)) (\phi_\eta^P(\bar{x}_3) + \phi_\eta^T(\bar{x}_3))] E'_a(t_c) h_{na}(x_1, x_2, x_3, b_1, b_3) \right. \\
& \left. - [x_3 \phi_V(\bar{x}_2)\phi_\eta^A(\bar{x}_3) + 4r_V r_\eta \phi_V^s(\bar{x}_2)\phi_\eta^P(\bar{x}_3) - r_V r_\eta (1-x_3) (\phi_V^s(\bar{x}_2) + \phi_V^t(\bar{x}_2)) \right. \\
& \left. \cdot (\phi_\eta^P(\bar{x}_3) - \phi_\eta^T(\bar{x}_3)) - r_V r_\eta x_2 (\phi_V^s(\bar{x}_2) - \phi_V^t(\bar{x}_2)) (\phi_\eta^P(\bar{x}_3) + \phi_\eta^T(\bar{x}_3))] \right. \\
& \left. \times E'_a(t'_c) h'_{na}(x_1, x_2, x_3, b_1, b_3) \right\}, \tag{17}
\end{aligned}$$

$$\begin{aligned}
M_{aV}^{P1} &= \frac{16}{\sqrt{3}} G_F \pi C_F m_B^4 \int_0^1 dx_1 dx_2 dx_3 \int_0^\infty b_1 db_1 b_3 db_3 \phi_B(x_1, b_1) \\
&\times \left\{ \left[(1-x_2) r_V \phi_\eta^A(\bar{x}_3) (\phi_V^s(\bar{x}_2) + \phi_V^t(\bar{x}_2)) - r_\eta x_3 \phi_V(\bar{x}_2) (\phi_\eta^P(\bar{x}_3) - \phi_\eta^T(\bar{x}_3)) \right] \right. \\
&\times E'_a(t_c) h_{na}(x_1, x_2, x_3, b_1, b_3) - \left. \left[-(x_2+1) r_V \phi_\eta^A(\bar{x}_3) (\phi_V^s(\bar{x}_2) + \phi_V^t(\bar{x}_2)) \right. \right. \\
&\left. \left. - r_\eta (x_3-2) \phi_V(\bar{x}_2) (\phi_\eta^P(\bar{x}_3) - \phi_\eta^T(\bar{x}_3)) \right] E'_a(t'_c) h'_{na}(x_1, x_2, x_3, b_1, b_3) \right\}, \quad (18)
\end{aligned}$$

$$\begin{aligned}
M_{aV}^{P2} &= \frac{16}{\sqrt{3}} G_F \pi C_F m_B^4 \int_0^1 dx_1 dx_2 dx_3 \int_0^\infty b_1 db_1 b_3 db_3 \phi_B(x_1, b_1) \{ [(x_2-1) \\
&\times \phi_V(\bar{x}_2) \phi_\eta^A(\bar{x}_3) - 4r_\eta r_V \phi_V^s(\bar{x}_2) \phi_\eta^P(\bar{x}_3) + r_\eta r_V x_2 (\phi_V^s(\bar{x}_2) + \phi_V^t(\bar{x}_2)) \\
&\cdot (\phi_\eta^P(\bar{x}_3) - \phi_\eta^T(\bar{x}_3)) + r_V r_\eta (1-x_3) (\phi_V^s(\bar{x}_2) - \phi_V^t(\bar{x}_2)) (\phi_\eta^P(\bar{x}_3) + \phi_\eta^T(\bar{x}_3))] \\
&\cdot E'_a(t_e) h_{na}(x_1, x_2, x_3, b_1, b_3) + [x_3 \phi_V(\bar{x}_2) \phi_\eta^A(\bar{x}_3) + x_3 r_V r_\eta (\phi_V^s(\bar{x}_2) + \phi_V^t(\bar{x}_2)) \\
&\cdot (\phi_\eta^P(\bar{x}_3) - \phi_\eta^T(\bar{x}_3)) + r_V r_\eta (1-x_2) (\phi_V^s(\bar{x}_2) - \phi_V^t(\bar{x}_2)) (\phi_\eta^P(\bar{x}_3) + \phi_\eta^T(\bar{x}_3))] \\
&\times E'_a(t'_e) h'_{na}(x_1, x_2, x_3, b_1, b_3) \}, \quad (19)
\end{aligned}$$

$$\begin{aligned}
F_e &= 4\sqrt{2} G_F \pi C_F m_B^4 \int_0^1 dx_1 dx_2 \int_0^\infty b_1 db_1 b_2 db_2 \phi_B(x_1, b_1) \\
&\times \left\{ \left[(1+x_2) \phi_\eta^A(\bar{x}_2) + (1-2x_2) r_\eta (\phi_\eta^P(\bar{x}_2) - \phi_\eta^T(\bar{x}_2)) \right] E_e(t_a) h_e(x_1, x_2, b_1, b_2) \right. \\
&\left. + 2r_\eta \phi_\eta^P(\bar{x}_2) E_e(t'_a) h_e(x_2, x_1, b_2, b_1) \right\}, \quad (20)
\end{aligned}$$

$$\begin{aligned}
M_e &= \frac{16}{\sqrt{3}} G_F \pi C_F m_B^4 \int_0^1 dx_1 dx_2 dx_3 \int_0^\infty b_1 db_1 b_3 db_3 \phi_B(x_1, b_1) \phi_V(\bar{x}_3) \\
&\times \left\{ -x_2 \phi_\eta^A(\bar{x}_2) - 2x_2 r_\eta \phi_\eta^T(\bar{x}_2) \right\} \cdot E'_e(t_b) h_n(x_1, x_2, x_3, b_1, b_3), \quad (21)
\end{aligned}$$

$$\begin{aligned}
M_e^{P1} &= -\frac{128}{\sqrt{6}} \pi C_F m_B^2 r_V \int_0^1 dx_1 dx_2 dx_3 \int_0^\infty b_1 db_1 b_3 db_3 \phi_B(x_1, b_1) \\
&\times \left\{ (1-x_3) \phi_\eta^A(\bar{x}_2) \cdot (\phi_V^s(\bar{x}_3) - \phi_V^t(\bar{x}_3)) \right. \\
&+ r_\eta (1-x_3) (\phi_\eta^P(\bar{x}_2) + \phi_\eta^T(\bar{x}_2)) (\phi_V^s(\bar{x}_3) - \phi_V^t(\bar{x}_3)) \\
&\left. + r_\eta x_2 (\phi_\eta^P(\bar{x}_2) - \phi_\eta^T(\bar{x}_2)) (\phi_V^s(\bar{x}_3) + \phi_V^t(\bar{x}_3)) \right\} \cdot E'_e(t_b) h_n(x_1, x_2, \bar{x}_3, b_1, b_3), \quad (22)
\end{aligned}$$

$$\begin{aligned}
M_a &= \frac{16}{\sqrt{3}} \sqrt{2} G_F \pi C_F m_B^4 \int_0^1 dx_1 dx_2 dx_3 \int_0^\infty b_1 db_1 b_3 db_3 \phi_B(x_1, b_1) \\
&\times \left\{ \left[(1-x_2) \phi_\eta^A(\bar{x}_2) \phi_V(\bar{x}_3) - r_\eta r_V (1-x_2) (\phi_\eta^P(\bar{x}_2) + \phi_\eta^T(\bar{x}_2)) (\phi_V^s(\bar{x}_3) - \phi_V^t(\bar{x}_3)) \right. \right. \\
&\left. \left. - r_\eta r_V x_3 (\phi_\eta^P(\bar{x}_2) - \phi_\eta^T(\bar{x}_2)) (\phi_V^s(\bar{x}_3) + \phi_V^t(\bar{x}_3)) \right] E'_a(t_c) h_{na}(x_1, x_2, x_3, b_1, b_3) \right. \\
&\left. - \left[x_3 \phi_\eta^A(\bar{x}_2) \phi_V(\bar{x}_3) - 4r_\eta r_V \phi_\eta^P(\bar{x}_2) \phi_V^s(\bar{x}_3) + r_\eta r_V (1-x_3) (\phi_\eta^P(\bar{x}_2) + \phi_\eta^T(\bar{x}_2)) \right. \right. \\
&\left. \left. \cdot (\phi_V^s(\bar{x}_3) - \phi_V^t(\bar{x}_3)) + r_\eta r_V x_2 (\phi_\eta^P(\bar{x}_2) - \phi_\eta^T(\bar{x}_2)) (\phi_V^s(\bar{x}_3) + \phi_V^t(\bar{x}_3)) \right] \right. \\
&\left. \times E'_a(t'_c) h'_{na}(x_1, x_2, x_3, b_1, b_3) \right\}, \quad (23)
\end{aligned}$$

$$\begin{aligned}
M_a^{P1} &= \frac{16}{\sqrt{3}} G_F \pi C_F m_B^4 \int_0^1 dx_1 dx_2 dx_3 \int_0^\infty b_1 db_1 b_3 db_3 \phi_B(x_1, b_1) \\
&\times \left\{ \left[-(1-x_2) r_\eta \phi_V(\bar{x}_3) (\phi_\eta^P(\bar{x}_2) + \phi_\eta^T(\bar{x}_2)) - r_V x_3 \phi_\eta^A(\bar{x}_2) (\phi_V^s(\bar{x}_3) - \phi_V^t(\bar{x}_3)) \right] \right. \\
&\times E'_a(t_c) h_{na}(x_1, x_2, x_3, b_1, b_3) - \left. \left[(x_2+1) r_\eta \phi_V(\bar{x}_3) (\phi_\eta^P(\bar{x}_2) + \phi_\eta^T(\bar{x}_2)) \right. \right. \\
&\left. \left. - r_V (x_3-2) \phi_\eta^A(\bar{x}_2) (\phi_V^s(\bar{x}_3) - \phi_V^t(\bar{x}_3)) \right] E'_a(t'_c) h'_{na}(x_1, x_2, x_3, b_1, b_3) \right\}, \quad (24)
\end{aligned}$$

$$\begin{aligned}
M_a^{P2} &= \frac{16}{\sqrt{3}} G_F \pi C_F m_B^4 \int_0^1 dx_1 dx_2 dx_3 \int_0^\infty b_1 db_1 b_3 db_3 \phi_B(x_1, b_1) \{ [(x_2-1) \\
&\times \phi_\eta^A(\bar{x}_2) \phi_V(\bar{x}_3) + 4 r_V r_\eta \phi_\eta^P(\bar{x}_2) \phi_V^s(\bar{x}_3) - r_V r_\eta x_2 (\phi_\eta^P(\bar{x}_2) + \phi_\eta^T(\bar{x}_2)) \\
&\cdot (\phi_V^s(\bar{x}_3) - \phi_V^t(\bar{x}_3)) - r_\eta r_V (1-x_3) (\phi_\eta^P(\bar{x}_2) - \phi_\eta^T(\bar{x}_2)) (\phi_V^s(\bar{x}_3) + \phi_V^t(\bar{x}_3))] \\
&\cdot E'_a(t_e) h_{na}(x_1, x_2, x_3, b_1, b_3) + [x_3 \phi_\eta^A(\bar{x}_2) \phi_V(\bar{x}_3) - x_3 r_\eta r_V (\phi_\eta^P(\bar{x}_2) + \phi_\eta^T(\bar{x}_2)) \\
&\cdot (\phi_V^s(\bar{x}_3) - \phi_V^t(\bar{x}_3)) - r_\eta r_V (1-x_2) (\phi_\eta^P(\bar{x}_2) - \phi_\eta^T(\bar{x}_2)) (\phi_V^s(\bar{x}_3) + \phi_V^t(\bar{x}_3))] \\
&\times E'_a(t'_e) h'_{na}(x_1, x_2, x_3, b_1, b_3) \}, \quad (25)
\end{aligned}$$

Here $r_V = m_V/m_B$ is the mass ratio with $(m_V = m_\rho, m_\omega, m_\phi)$; $C_F = 4/3$ is a color factor. The evolution functions $E(t_i)$ and hard function $h_j(x_i, b_i)$ are displayed in Appendix B.

The decay amplitudes for $B \rightarrow \rho\eta'$, $B^0 \rightarrow \omega\eta'$, and $B^0 \rightarrow \phi\eta'$ decays can be obtained easily from Eqs.(8) to (11) by the following replacements

$$f_\eta^q, f_\eta^s \longrightarrow f_{\eta'}^q, f_{\eta'}^s, \quad (26)$$

$$F_1(\phi) \longrightarrow F'_1(\phi) = \frac{1}{\sqrt{2}} \sin \phi, \quad (27)$$

$$F_2(\phi) \longrightarrow F'_2(\phi) = \cos \phi. \quad (28)$$

IV. NEXT-TO-LEADING CONTRIBUTIONS

The power counting in the pQCD approach [15] is different from that in the QCDF approach[3]. Here the term NLO means that the decay amplitude is proportional to $\alpha_s^2(\mu)$. We here indeed consider the partial NLO contributions only: those from the vertex corrections, the quark-loops and chromo-magnetic penguins. The NLO contributions from hard-spectator and annihilation diagrams are not known at present. When compared with the previous LO calculations in pQCD [12], the following NLO contributions will be included:

1. The LO Wilson coefficients $C_i(m_W)$ will be replaced by those at NLO level in NDR scheme [18]. As mentioned in last section, the strong coupling constant $\alpha_s(t)$ at two-loop level as given in Eq. (7), and the NLO RG evolution matrix $U(t, m, \alpha)$, as defined in Ref. [18], will be used here:

$$U(m_1, m_2, \alpha) = U(m_1, m_2) + \frac{\alpha}{4\pi} R(m_1, m_2) \quad (29)$$

where the function $U(m_1, m_2)$ and $R(m_1, m_2)$ represent the QCD and QED evolution and have been defined in Eq. (6.24) and (7.22) in Ref. [18]. We also introduce a cut-off $\mu_0 = 1$ GeV for the hard scale “t” in the final integration.

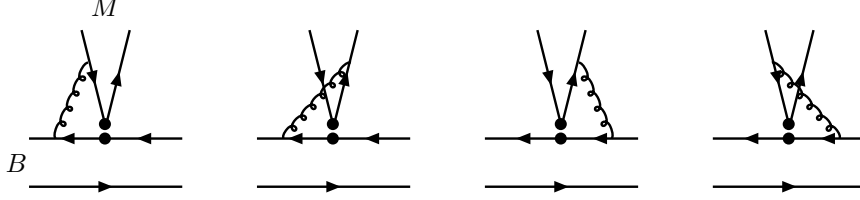


FIG. 2: NLO vertex corrections to the factorizable amplitudes.

A. Vertex corrections

The vertex corrections to the factorizable emission diagrams, as illustrated by Fig. 2, have been calculated years ago in the QCD factorization approach [3, 19]. According to Ref. [15], the difference of the calculations induced by considering or not considering the parton transverse momentum is rather small, say less than 10%, and therefore can be neglected. Consequently, one can use the vertex corrections as given in Ref. [19] directly. The vertex corrections can be absorbed into the re-definition of the Wilson coefficients $a_i(\mu)$ by adding a vertex-function $V_i(M)$ to them [3, 19]

$$\begin{aligned}
 a_i(\mu) &\rightarrow a_i(\mu) + \frac{\alpha_s(\mu)}{4\pi} C_F \frac{C_i(\mu)}{3} V_i(M), \quad \text{for } i = 1, 2; \\
 a_j(\mu) &\rightarrow a_j(\mu) + \frac{\alpha_s(\mu)}{4\pi} C_F \frac{C_{j\pm 1}(\mu)}{N_c} V_j(M), \quad \text{for } j = 3 - 10,
 \end{aligned} \tag{30}$$

where M is the meson emitted from the weak vertex. When M is a pseudo-scalar meson, the vertex functions $V_i(M)$ are given (in the NDR scheme) in Refs. [15, 19]:

$$V_i(M) = \begin{cases} 12 \ln \frac{m_b}{\mu} - 18 + \frac{2\sqrt{2N_c}}{f_M} \int_0^1 dx \phi_M^A(x) g(x), & \text{for } i = 1 - 4, 9, 10, \\ -12 \ln \frac{m_b}{\mu} + 6 - \frac{2\sqrt{2N_c}}{f_M} \int_0^1 dx \phi_M^A(x) g(1-x), & \text{for } i = 5, 7, \\ -6 + \frac{2\sqrt{2N_c}}{f_M} \int_0^1 dx \phi_M^P(x) h(x), & \text{for } i = 6, 8, \end{cases} \tag{31}$$

where f_M is the decay constant of the meson M ; $\phi_M^A(x)$ and $\phi_M^P(x)$ are the twist-2 and twist-3 distribution amplitude of the meson M , respectively. For a vector meson V , $\phi_M^A(\phi_M^P)$ is replaced by $\phi_V(\phi_V^s)$ and f_M by f_V^T in the third line of the above formulas. The hard-scattering functions $g(x)$ and $h(x)$ in Eq. (31) are:

$$\begin{aligned}
 g(x) &= 3 \left(\frac{1-2x}{1-x} \ln x - i\pi \right) \\
 &\quad + \left[2Li_2(x) - \ln^2 x + \frac{2 \ln x}{1-x} - (3 + 2i\pi) \ln x - (x \leftrightarrow 1-x) \right], \tag{32}
 \end{aligned}$$

$$h(x) = 2Li_2(x) - \ln^2 x - (1 + 2i\pi) \ln x - (x \leftrightarrow 1-x), \tag{33}$$

where $Li_2(x)$ is the dilogarithm function. As shown in Ref. [15], the μ -dependence of the Wilson coefficients $a_i(\mu)$ will be improved generally by the inclusion of the vertex corrections.

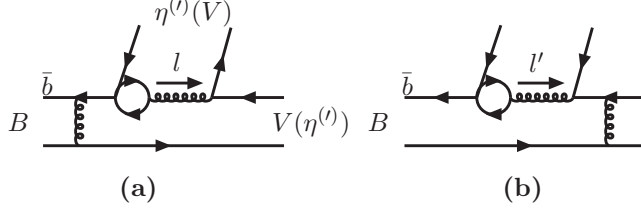


FIG. 3: Quark-loop diagrams contributing to $B \rightarrow \rho(\omega)\eta^{(l)}$ decays.

B. Quark loops

The contribution from the so-called “quark-loops” is a kind of penguin correction with the four quark operators insertion, as illustrated by Fig. 3. In fact this is generally called BSS mechanism[20], which plays a very important role in producing the CP violation in the QCDF/SCET approaches. We here include quark-loop amplitude from the operators $O_{1,2}$ and O_{3-6} only. The quark loops from O_{7-10} will be neglected due to their smallness.

For the $b \rightarrow d$ transition, the contributions from the various quark loops are described by the effective Hamiltonian $H_{eff}^{(ql)}$ [15],

$$H_{eff}^{(ql)} = - \sum_{q=u,c,t} \sum_{q'} \frac{G_F}{\sqrt{2}} V_{qb} V_{qd}^* \frac{\alpha_s(\mu)}{2\pi} C^{(q)}(\mu, l^2) (\bar{d}\gamma_\rho (1 - \gamma_5) T^a b) (\bar{q}'\gamma^\rho T^a q'), \quad (34)$$

where l^2 being the invariant mass of the gluon, which connects the quark loops with the $\bar{q}'q$ pair as shown in Fig. 3. The functions $C^{(q)}(\mu, l^2)$ can be written as

$$C^{(q)}(\mu, l^2) = \left[G^{(q)}(\mu, l^2) - \frac{2}{3} \right] C_2(\mu), \quad (35)$$

for $q = u, c$ and

$$C^{(t)}(\mu, l^2) = \left[G^{(s)}(\mu, l^2) - \frac{2}{3} \right] C_3(\mu) + \sum_{q''=u,d,s,c} G^{(q'')}(\mu, l^2) [C_4(\mu) + C_6(\mu)]. \quad (36)$$

The integration function $G^{(q)}(\mu, l^2)$ for the loop of the quarks $q = (u, d, s, c)$ is defined as [15]

$$G^{(q)}(\mu, l^2) = -4 \int_0^1 dx x(1-x) \ln \frac{m_q^2 - x(1-x)l^2}{\mu^2}, \quad (37)$$

where m_q is the quark mass. The explicit expressions of the function $G^{(q)}(\mu, l^2)$ after the integration can be found, for example, in Ref. [15].

It is straightforward to calculate the decay amplitude for Fig.3a and 3b. For the case of $B \rightarrow V$ or $B \rightarrow \eta$ transition, we find two kinds of topological decay amplitudes:

$$M_{V\eta}^{(q)} = -16m_B^2 \frac{C_F^2}{\sqrt{2N_c}} \int_0^1 dx_1 dx_2 dx_3 \int_0^\infty b_1 db_1 b_2 db_2 \phi_B(x_1, b_1) \left\{ [(1+x_2)\phi_V(\bar{x}_2)\phi_\eta^A(\bar{x}_3) - r_V(1-2x_2)(\phi_V^s(\bar{x}_2) - \phi_V^t(\bar{x}_2))\phi_\eta^A(\bar{x}_3) - 2r_\eta\phi_V(\bar{x}_2)\phi_\eta^P(\bar{x}_3) + 2r_V r_\eta((2+x_2)\cdot\phi_V^s(\bar{x}_2) + x_2\phi_V^t(\bar{x}_2))\phi_\eta^P(\bar{x}_3)] E^{(q)}(t_q, l^2) h_e(x_2, x_1, b_2, b_1) + [-2r_V\phi_V^s(\bar{x}_2)\phi_\eta^A(\bar{x}_3) + 4r_V r_\eta\phi_V^s(\bar{x}_2)\phi_\eta^P(\bar{x}_3)] E^{(q)}(t'_q, l'^2) h_e(x_1, x_2, b_1, b_2) \right\}, \quad (38)$$

for $B \rightarrow V$ transition, and

$$\begin{aligned}
M_{\eta V}^{(q)} = & -\frac{4}{\sqrt{3}}G_F C_F^2 m_B^4 \int_0^1 dx_1 dx_2 dx_3 \int_0^\infty b_1 db_1 b_2 db_2 \phi_B(x_1, b_1) \{ [(1+x_2)\phi_\eta^A(\bar{x}_2)\phi_V(\bar{x}_3) \\
& + r_\eta(1-2x_2)(\phi_\eta^P(\bar{x}_2) - \phi_\eta^T(\bar{x}_2))\phi_V(\bar{x}_3) - 2r_V\phi_\eta^A(\bar{x}_2)\phi_V^s(\bar{x}_3) - 2r_\eta r_V((2+x_2) \\
& \cdot \phi_\eta^P(\bar{x}_2) + x_2\phi_\eta^T(\bar{x}_2))\phi_V^s(\bar{x}_3)] E^{(q)}(t_q, l^2) h_e(x_2, x_1, b_2, b_1) + [2r_\eta\phi_\eta^P(\bar{x}_2)\phi_V(\bar{x}_3) \\
& - 4r_\eta r_V\phi_\eta^P(\bar{x}_2)\phi_V^s(\bar{x}_3)] E^{(q)}(t'_q, l'^2) h_e(x_1, x_2, b_1, b_2) \}, \tag{39}
\end{aligned}$$

for $B \rightarrow \eta$ transition. Here V represents ρ, ω , or ϕ meson, and $r_\eta = m_\eta/m_B, r_V = m_V/m_B$. The evolution factors take the form of

$$E^{(q)}(t, l^2) = C^{(q)}(t, l^2) \alpha_s^2(t) \cdot \exp[-S_{ab}], \tag{40}$$

with the Sudakov factor S_{ab} and the hard function $h_e(x_1, x_2, b_1, b_2)$ as given in Eq. (B9) and Eq. (B2) respectively, and finally the hard scales and the gluon invariant masses are

$$\begin{aligned}
t_q &= \max(\sqrt{x_2}m_B, \sqrt{x_1 x_2}m_B, \sqrt{(1-x_2)x_3}m_B, 1/b_1, 1/b_2); \\
t'_q &= \max(\sqrt{x_1}m_B, \sqrt{x_1 x_2}m_B, \sqrt{|x_3 - x_1|}m_B, 1/b_1, 1/b_2), \tag{41}
\end{aligned}$$

$$\begin{aligned}
l^2 &= (1-x_2)x_3m_B^2 - |\mathbf{k}_{2T} - \mathbf{k}_{3T}|^2 \approx (1-x_2)x_3m_B^2, \\
l'^2 &= (x_3-x_1)m_B^2 - |\mathbf{k}_{1T} - \mathbf{k}_{3T}|^2 \approx (x_3-x_1)m_B^2. \tag{42}
\end{aligned}$$

For $B \rightarrow V\eta'$ decays, we find the similar results by making appropriate replacements, such as $r_\eta \rightarrow r - \eta'$, etc.

Finally, the total ‘‘quark-loop’’ contribution to the considered $B \rightarrow V\eta^{(\prime)}$ decays with $V = \rho, \omega$ can be written as

$$M_{V\eta^{(\prime)}}^{(q)} = \langle V\eta^{(\prime)} | \mathcal{H}_{eff}^q | B \rangle = \sum_{q=u,c,t} \lambda_q [M_{V\eta^{(\prime)}}^{(q)} + M_{\eta^{(\prime)}V}^{(q)}], \tag{43}$$

where $\lambda_q = V_{qb}V_{qd}^*$. The quark-loops do not contribute to $B \rightarrow \phi\eta^{(\prime)}$ decays.

It is note that the quark-loop corrections are mode dependent. The assumption of a constant gluon invariant mass in FA introduces a large theoretical uncertainty as making predictions. In the PQCD approach, the gluon invariant mass is related to the parton momenta unambiguously.

C. Magnetic penguins

As illustrated by Fig. 4, the chromo-magnetic penguin operator O_{8g} also contribute to $B \rightarrow V\eta^{(\prime)}$ decays at NLO level. The corresponding weak effective Hamiltonian contains the $b \rightarrow dg$ transition,

$$\mathcal{H}_{eff}^{cmp} = -\frac{G_F}{\sqrt{2}} V_{tb} V_{td}^* C_{8g}^{eff} O_{8g}, \tag{44}$$

with the chromo-magnetic penguin operator,

$$O_{8g} = \frac{g_s}{8\pi^2} m_b \bar{d}_i \sigma^{\mu\nu} (1 + \gamma_5) T_{ij}^a G_{\mu\nu}^a b_j, \tag{45}$$

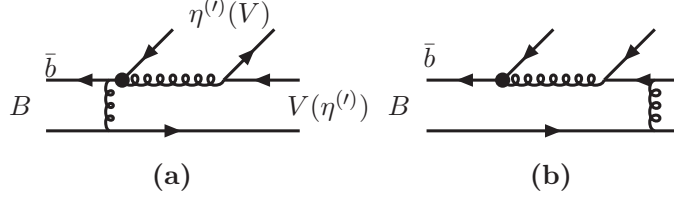


FIG. 4: Chromo-Magnetic penguin (O_{8g}) diagrams contributing to $B \rightarrow \rho(\omega)\eta^{(\prime)}$ decays.

where i, j being the color indices of quarks. The corresponding effective Wilson coefficient $C_{8g}^{eff} = C_{8g} + C_5$ [15].

In Ref. [21], the authors calculated the chromo-magnetic penguin contributions to $B \rightarrow \phi K$ decays using the pQCD approach. They considered nine chromo-magnetic penguin diagrams corresponding to the non-local operator O'_{8g} , as given in Eq. (2.3) of Ref. [21], generated by operator O_{8g} as defined in Eq. (45). The first two Feynman diagrams (a) and (b) in Ref. [21] are the same as Figs. 4a and 4b here. According to Ref. [21], the diagrams (a) and (b) dominate, while other seven diagrams are small or negligible. It is therefore reasonable for us to consider the NLO contributions induced by the diagrams (a) and (b) only, for the sake of simplicity.

The decay amplitude for Figs. 4a and 4b can be written as

$$\begin{aligned}
M_{V\eta}^{(g)} = & 16m_B^4 \frac{C_F^2}{2\sqrt{N_c}} \int_0^1 dx_1 dx_2 dx_3 \int_0^\infty b_1 db_1 b_2 db_2 \phi_B(x_1, b_1) \{ [-(1-x_2) \{ 2\phi_V(\bar{x}_2) - r_V \\
& \cdot (3\phi_V^s(\bar{x}_2) - \phi_V^t(\bar{x}_2)) - r_V x_2 (\phi_V^s(\bar{x}_2) + \phi_V^t(\bar{x}_2)) \} \phi_\eta^A(\bar{x}_3) + r_\eta (1+x_2) x_3 \phi_V(\bar{x}_2) \\
& \cdot (3\phi_\eta^P(\bar{x}_3) + \phi_\eta^T(\bar{x}_3)) - r_V r_\eta (1-x_2) (\phi_V^s(\bar{x}_2) + \phi_V^t(\bar{x}_2)) (3\phi_\eta^P(\bar{x}_3) - \phi_\eta^T(\bar{x}_3)) \\
& - r_V r_\eta x_3 (1-2x_2) (\phi_V^s(\bar{x}_2) - \phi_V^t(\bar{x}_2)) (3\phi_\eta^P(\bar{x}_3) + \phi_\eta^T(\bar{x}_3))] \\
& \cdot E_g(t_q) h_g(A, B, C, b_1, b_2, b_3, x_2) - E_g(t'_q) h_g(A', B', C', b_2, b_1, b_3, x_1) \\
& \cdot [-4r_V \phi_V^s(\bar{x}_2) \phi_\eta^A(\bar{x}_3) + 2r_V r_\eta x_3 \phi_V^s(\bar{x}_2) (3\phi_\eta^P(\bar{x}_3) + \phi_\eta^T(\bar{x}_3))] \}, \quad (46)
\end{aligned}$$

for the case of $B \rightarrow V$ transition, and

$$\begin{aligned}
M_{\eta V}^{(g)} = & \frac{4}{\sqrt{3}} G_F C_F^2 m_B^6 \int_0^1 dx_1 dx_2 dx_3 \int_0^\infty b_1 db_1 b_2 db_2 \phi_B(x_1, b_1) \{ [-(1-x_2) \{ 2\phi_\eta^A(\bar{x}_2) + r_\eta \\
& \cdot (3\phi_\eta^P(\bar{x}_2) - \phi_\eta^T(\bar{x}_2)) + r_\eta x_2 (\phi_\eta^P(\bar{x}_2) + \phi_\eta^T(\bar{x}_2)) \} \phi_V(\bar{x}_3) + r_V (1+x_2) x_3 \phi_\eta^A(\bar{x}_2) \\
& \cdot (3\phi_V^s(\bar{x}_3) + \phi_V^t(\bar{x}_3)) + r_\eta r_V (1-x_2) (\phi_\eta^P(\bar{x}_2) + \phi_\eta^T(\bar{x}_2)) (3\phi_V^s(\bar{x}_3) - \phi_V^t(\bar{x}_3)) \\
& + r_\eta r_V x_3 (1-2x_2) (\phi_\eta^P(\bar{x}_2) - \phi_\eta^T(\bar{x}_2)) (3\phi_V^s(\bar{x}_3) + \phi_V^t(\bar{x}_3))] \\
& \cdot E_g(t_q) h_g(A, B, C, b_1, b_2, b_3, x_2) - E_g(t'_q) h_g(A', B', C', b_2, b_1, b_3, x_1) \\
& \cdot [4r_\eta \phi_\eta^P(\bar{x}_2) \phi_V(\bar{x}_3) - 2r_\eta r_V x_3 \phi_\eta^P(\bar{x}_2) (3\phi_V^s(\bar{x}_3) + \phi_V^t(\bar{x}_3))] \}. \quad (47)
\end{aligned}$$

for the case of $B \rightarrow \eta$ transition. Here the hard scale t_q and t'_q are the same as in Eq. (41). The evolution factor $E_g(t)$ in Eqs. (46) and (47) is of the form

$$E_g(t) = C_{8g}^{eff}(t) \alpha_s^2(t) \cdot \exp[-S_{mg}], \quad (48)$$

with the Sudakov factor S_{mg} and the hard function h_g ,

$$\begin{aligned}
S_{mg}(t) = & s\left(x_1 m_B / \sqrt{2}, b_1\right) + s\left(x_2 m_B / \sqrt{2}, b_2\right) + s\left((1-x_2) m_B / \sqrt{2}, b_2\right) \\
& + s\left(x_3 m_B / \sqrt{2}, b_3\right) + s\left((1-x_3) m_B / \sqrt{2}, b_3\right) \\
& - \frac{1}{\beta_1} \left[\ln \frac{\ln(t/\Lambda)}{-\ln(b_1 \Lambda)} + \ln \frac{\ln(t/\Lambda)}{-\ln(b_2 \Lambda)} + \ln \frac{\ln(t/\Lambda)}{-\ln(b_3 \Lambda)} \right], \tag{49}
\end{aligned}$$

$$\begin{aligned}
h_g(A, B, C, b_1, b_2, b_3, x_i) = & -S_t(x_i) K_0(Bb_1) K_0(Cb_3) \\
& \cdot \int_0^{\pi/2} d\theta \tan \theta \cdot J_0(Ab_1 \tan \theta) J_0(Ab_2 \tan \theta) J_0(Ab_3 \tan \theta), \tag{50}
\end{aligned}$$

where the functions $K_0(x)$ and $J_0(x)$ are the Bessel functions, the form factor $S_t(x_i)$ with $i = 1, 2$ has been given in Eq. (B7), and the invariant masses $A^{(\prime)}, B^{(\prime)}$ and $C^{(\prime)}$ of the virtual quarks and gluons are of the form

$$\begin{aligned}
A = \sqrt{x_2} m_B, \quad B = B' = \sqrt{x_1 x_2} m_B, \quad C = i \sqrt{(1-x_2) x_3} m_B, \\
A' = \sqrt{x_1} m_B, \quad C' = \sqrt{|x_1 - x_3|} m_B. \tag{51}
\end{aligned}$$

For $B \rightarrow V\eta'$ decays, we find the similar results by making appropriate replacements.

The total ‘‘chromo-magnetic penguin’’ contribution to the considered $B \rightarrow V\eta^{(\prime)}$ decays can therefore be written as

$$M_{V\eta^{(\prime)}}^{(cmp)} = \langle V\eta^{(\prime)} | \mathcal{H}_{eff}^{cmp} | B \rangle = \lambda_t \left[M_{V\eta^{(\prime)}}^{(g)} + M_{\eta^{(\prime)}V}^{(g)} \right], \tag{52}$$

where $\lambda_t = V_{tb} V_{td}^*$. Again, the chromo-magnetic penguins do not contribute to $B \rightarrow \phi\eta^{(\prime)}$ decays.

V. NUMERICAL RESULTS AND DISCUSSIONS

Using the wave functions and the central values of relevant input parameters as given in Appendix A, we firstly find the numerical values of the corresponding form factors at zero momentum transfer:

$$\begin{aligned}
A_0^{B \rightarrow \rho}(q^2 = 0) &= 0.32_{-0.04}^{+0.05}(\omega_b), \\
A_0^{B \rightarrow \omega}(q^2 = 0) &= 0.29_{-0.03}^{+0.04}(\omega_b), \\
F_0^{B \rightarrow \eta^{(\prime)}}(q^2 = 0) &= 0.22 \pm 0.03(\omega_b), \tag{53}
\end{aligned}$$

for $\omega_b = 0.40 \pm 0.04 \text{ GeV}$, which agree well with those obtained in QCD sum rule calculations.

A. Branching ratios

For a general charmless two-body decays $B \rightarrow V\eta^{(\prime)}$, the branching ratio can be written in general as

$$Br(B \rightarrow V\eta^{(\prime)}) = \tau_B \frac{1}{16\pi m_B} |\mathcal{M}|^2 \quad (54)$$

where τ_B is the lifetime of the B meson, and the decay amplitude is the form of

$$\mathcal{M} = \langle V\eta^{(\prime)} | \mathcal{H}_{eff} + \mathcal{H}_{eff}^{(ql)} + \mathcal{H}_{eff}^{(cmp)} | B \rangle . \quad (55)$$

Using the wave functions and the input parameters as specified in previous sections, it is straightforward to calculate the CP-averaged branching ratios for the considered decays, which are listed in Table I. For comparison, we also list the corresponding updated experimental results [22, 23] and numerical results evaluated in the framework of the QCD factorization (QCDF) [19].

TABLE I: The pQCD predictions for the branching ratios (in unit of 10^{-6}). The label LO_{NLOWC} means the LO results with the NLO Wilson coefficients, and +VC, +QL, +MP, NLO means the inclusion of the vertex corrections, the quark loops, the magnetic penguin, and all the considered NLO corrections, respectively.

Mode	LO	LO_{NLOWC}	+VC	+QL	+MP	NLO	Data	QCDF
$B^\pm \rightarrow \rho^\pm \eta$	6.9	7.4	6.8	7.5	7.2	6.7	5.4 ± 1.2	$9.4^{+5.9}_{-4.8}$
$B^\pm \rightarrow \rho^\pm \eta'$	5.2	4.8	4.6	4.9	4.7	4.6	$9.1^{+3.7}_{-2.8}$	$6.3^{+4.0}_{-3.3}$
$B^0 \rightarrow \rho^0 \eta$	0.08	0.08	0.19	0.16	0.12	0.13	< 1.5	$0.03^{+0.17}_{-0.10}$
$B^0 \rightarrow \rho^0 \eta'$	0.05	0.04	0.13	0.06	0.04	0.10	< 1.3	$0.01^{+0.12}_{-0.06}$
$B^0 \rightarrow \omega \eta$	0.22	0.34	0.67	0.33	0.25	0.71	< 1.9	$0.31^{+0.46}_{-0.27}$
$B^0 \rightarrow \omega \eta'$	0.12	0.18	0.52	0.19	0.15	0.55	< 2.2	$0.20^{+0.34}_{-0.18}$
$B^0 \rightarrow \phi \eta$	0.001	0.002	0.011	-	-	0.011	< 0.6	0.001
$B^0 \rightarrow \phi \eta'$	0.096	0.053	0.017	-	-	0.017	< 0.5	0.001

It is worth stressing that the theoretical predictions in the pQCD approach still have relatively large theoretical errors induced by the large uncertainties of many input parameters, such as ω_b , Gegenbauer coefficient a_2 , the CKM angle α and m_s . The pQCD predictions with the major theoretical errors for the branching ratios of the decays under

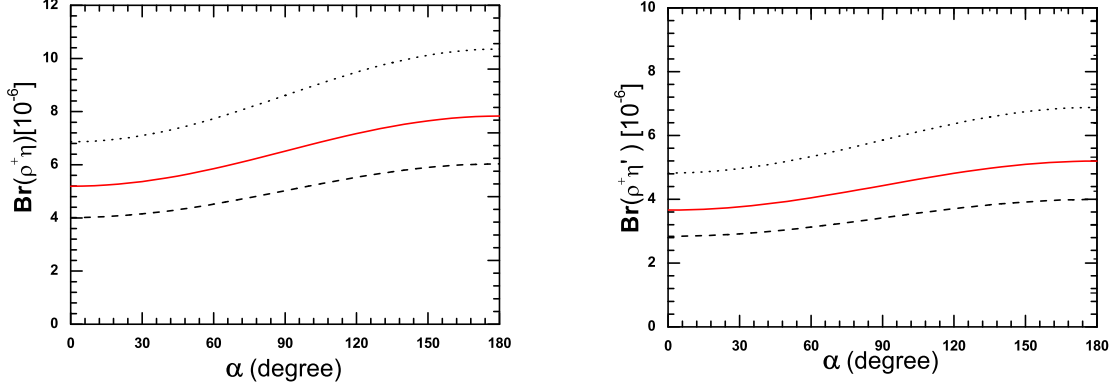


FIG. 5: The α dependence of the branching ratios of $B^+ \rightarrow \rho^+ \eta^{(\prime)}$ decays for $\omega_b = 0.36$ GeV (dotted curve), 0.40 GeV (solid curve) and 0.44 GeV (dashed curve).

consideration are the following

$$\begin{aligned}
Br(B^\pm \rightarrow \rho^\pm \eta) &= [6.7_{-1.5}^{+2.2}(\omega_b)_{-0.9}^{+1.0}(\mu_0)_{-0.4}^{+0.5}(\alpha)_{-0.5}^{+0.7}(a_2)_{-0.0}^{+0.1}(a_{2\rho})] \times 10^{-6}, \\
Br(B^\pm \rightarrow \rho^\pm \eta') &= [4.6_{-1.1}^{+1.4}(\omega_b)_{-0.7}^{+0.5}(\mu_0)_{-0.3}^{+0.2}(\alpha) \pm 0.4(a_2)_{-0.1}^{+0.0}(a_{2\rho})] \times 10^{-6}, \\
Br(B^0 \rightarrow \rho^0 \eta) &= [1.3_{-0.2}^{+0.4}(\omega_b)_{-0.4}^{+1.1}(\mu_0)_{-0.0}^{+0.1}(\alpha)_{-0.0}^{+0.1}(a_2)_{-0.1}^{+0.2}(a_{2\rho})] \times 10^{-7}, \\
Br(B^0 \rightarrow \rho^0 \eta') &= [1.0_{-0.2}^{+0.3}(\omega_b)_{-0.4}^{+0.3}(\mu_0) \pm 0.2(\alpha)_{-0.1}^{+0.0}(a_2) \pm 0.1(a_{2\rho})] \times 10^{-7}, \\
Br(B^0 \rightarrow \omega \eta) &= [7.1_{-1.3}^{+1.7}(\omega_b)_{-1.8}^{+2.6}(\mu_0)_{-0.2}^{+0.1}(\alpha)_{-1.4}^{+1.7}(a_2)_{-0.8}^{+1.0}(a_{2\omega})] \times 10^{-7}, \\
Br(B^0 \rightarrow \omega \eta') &= [5.5_{-1.1}^{+1.3}(\omega_b)_{-1.6}^{+2.1}(\mu_0)_{-1.0}^{+1.2}(\alpha)_{-1.2}^{+1.3}(a_2)_{-0.7}^{+0.8}(a_{2\omega})] \times 10^{-7}, \\
Br(B^0 \rightarrow \phi \eta) &= [1.1 \pm 0.1(\omega_b)_{-0.8}^{+5.9}(\mu_0)_{-0.2}^{+0.4}(m_s)_{-0.2}^{+0.1}(a_2)_{-0.28}^{+0.30}(a_{2\phi})] \times 10^{-8}, \\
Br(B^0 \rightarrow \phi \eta') &= [1.7 \pm 0.2(\omega_b)_{-0.9}^{+15.3}(\mu_0)_{-0.4}^{+0.9}(m_s) \pm 0.1(a_2) \pm 0.1(a_{2\phi})] \times 10^{-8}, \quad (56)
\end{aligned}$$

where the major errors are induced by the uncertainties of $\omega_b = 0.4 \pm 0.04$ GeV, $\mu_0 = 1.0 \pm 0.5$ GeV, $\alpha = 100^\circ \pm 20^\circ$, $m_s = 130 \pm 30$ MeV, Gegenbauer coefficients $a_2 = 0.115 \pm 0.115$, $a_{2\rho} = a_{2\omega} = 0.15 \pm 0.15$ and $a_{2\phi} = 0.2 \pm 0.2$, respectively.

In Figs. 5, 6 and 7 we show the α and ω_b -dependence of the pQCD predictions for the branching ratios of $B \rightarrow \rho \eta^{(\prime)}$, $B \rightarrow \omega \eta^{(\prime)}$ decays for $\omega_b = 0.4 \pm 0.04$ GeV, and $\alpha = [0^\circ, 180^\circ]$, $a_2 = 0.115$ and $a_{2\rho} = a_{2\omega} = 0.15$.

From the numerical results and the figures, we observe that

- For $B^\pm \rightarrow \rho^\pm \eta$ decay, the inclusion of the considered NLO corrections can improve the agreement between the pQCD prediction and the data. But for $B^\pm \rightarrow \rho^\pm \eta'$ decay, we are not so lucky. Although the pQCD predictions for $Br(B^\pm \rightarrow \rho^\pm \eta^{(\prime)})$ agree with the data within one standard deviation, but the predicted pattern of $Br(B^\pm \rightarrow \rho^\pm \eta) > Br(B^\pm \rightarrow \rho^\pm \eta')$ in both the pQCD and QCDF is contrary to the observed one.
- For $B^0 \rightarrow \rho^0(\omega, \phi) \eta^{(\prime)}$ decays, the pQCD predictions for their Br's are consistent with currently available upper limits. Except for $Br(B \rightarrow \phi \eta')$, the inclusion of the

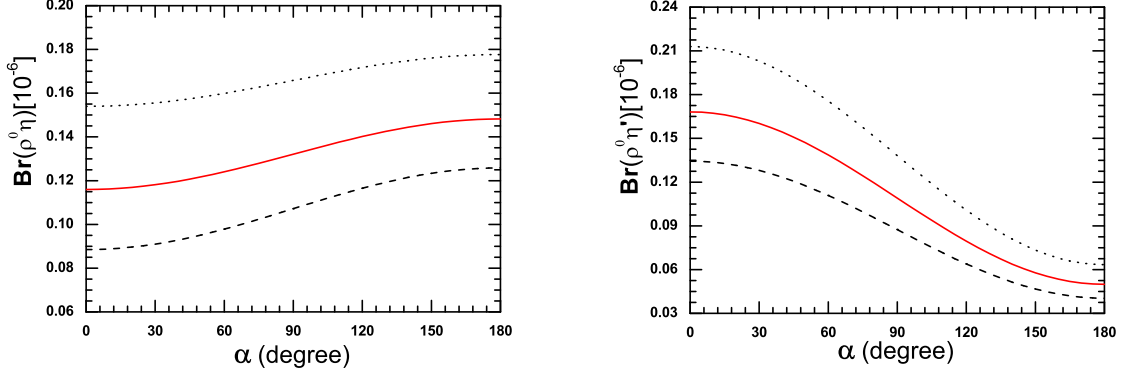


FIG. 6: The α dependence of the branching ratios (in units of 10^{-6}) of $B^0 \rightarrow \rho^0 \eta^{(\prime)}$ decays for $\omega_b = 0.36$ GeV (dotted curve), 0.40 GeV (solid curve) and 0.44 GeV (dashed curve).

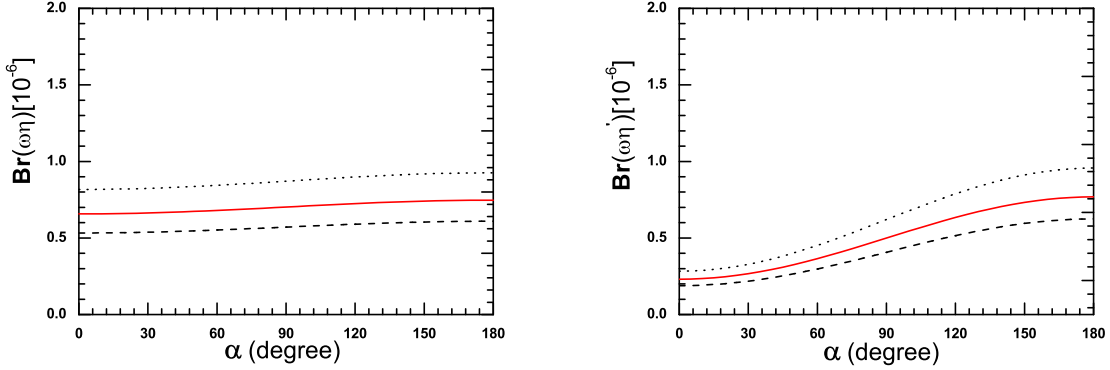


FIG. 7: The α dependence of the branching ratios (in units of 10^{-6}) of $B^0 \rightarrow \omega \eta^{(\prime)}$ decays for $\omega_b = 0.36$ GeV (dotted curve), 0.40 GeV (solid curve) and 0.44 GeV (dashed curve).

partial NLO contributions to other decays can enhance their Br's by a factor of two to ten, and generally larger than the QCDF predictions, which will be tested by the forthcoming LHCb experiment.

B. CP-violating asymmetries

Now we turn to the evaluations of the CP-violating asymmetries of $B \rightarrow \rho(\omega, \phi) \eta^{(\prime)}$ decays in pQCD approach. For $B^+ \rightarrow \rho^+ \eta$ and $B^+ \rightarrow \rho^+ \eta'$ decays, the direct CP-violating

asymmetries \mathcal{A}_{CP} can be defined as:

$$\mathcal{A}_{CP}^{dir} = \frac{|\overline{\mathcal{M}}_f|^2 - |\mathcal{M}_f|^2}{|\overline{\mathcal{M}}_f|^2 + |\mathcal{M}_f|^2}, \quad (57)$$

The pQCD predictions for the direct CP-violating asymmetries of $B^\pm \rightarrow \rho^\pm \eta^{(\prime)}$ decays are listed in Table II. For comparison, we also list currently available experimental results [22, 23] and the numerical results evaluated in the framework of the QCD factorization (QCDF) [19].

TABLE II: The pQCD predictions for the direct CP-violating asymmetries of $B^\pm \rightarrow \rho^\pm \eta^{(\prime)}$ decays (in units of 10^{-2}).

Mode	LO	+VC	+QL	+MP	NLO	Data	QCDF
$\mathcal{A}_{CP}^{dir}(B^\pm \rightarrow \rho^\pm \eta)$	0.0	1.3	1.4	-0.1	1.9	1.0 ± 16.0	2.4
$\mathcal{A}_{CP}^{dir}(B^\pm \rightarrow \rho^\pm \eta')$	-6.8	-25.3	-5.7	-7.1	-25.0	-4.0 ± 28	-4.1

The NLO pQCD predictions for the central values of the direct CP-violating asymmetries and the major theoretical errors for $B^\pm \rightarrow \rho^\pm \eta^{(\prime)}$ decays are

$$\mathcal{A}_{CP}^{dir}(B^\pm \rightarrow \rho^\pm \eta) = [1.9_{-0.0}^{+0.1}(\omega_b)_{-0.3}^{+0.2}(\alpha)_{-0.0}^{+0.1}(a_2)_{-0.5}^{+0.6}(a_{2\rho})] \times 10^{-2}, \quad (58)$$

$$\mathcal{A}_{CP}^{dir}(B^\pm \rightarrow \rho^\pm \eta') = [-25.0_{-0.3}^{+0.4}(\omega_b)_{-1.6}^{+4.1}(\alpha)_{-0.7}^{+0.8}(a_2)_{-1.8}^{+2.1}(a_{2\rho})] \times 10^{-2}, \quad (59)$$

where the major theoretical errors come from the variations of $\omega_b = 0.4 \pm 0.04$ GeV, $\alpha = 100^\circ \pm 20^\circ$, Gegenbauer coefficients $a_2 = 0.115 \pm 0.115$, $a_{2\rho} = a_{2\omega} = 0.15 \pm 0.15$. Both the pQCD and QCDF predictions are consistent with the data because of the still large theoretical and experimental errors. In Fig. 8, one shows the α and ω_b -dependence of the LO and NLO pQCD predictions for the CP-violating asymmetries of $B^\pm \rightarrow \rho^\pm \eta^{(\prime)}$.

As to the CP-violating asymmetries for the neutral decays $B^0 \rightarrow \rho^0(\omega)\eta^{(\prime)}$, the effects of $B^0 - \bar{B}^0$ mixing should be considered. The CP-violating asymmetries for such decays are time dependent and can be defined as

$$\begin{aligned} A_{CP} &\equiv \frac{\Gamma(\overline{B}_d^0(\Delta t) \rightarrow f_{CP}) - \Gamma(B_d^0(\Delta t) \rightarrow f_{CP})}{\Gamma(\overline{B}_d^0(\Delta t) \rightarrow f_{CP}) + \Gamma(B_d^0(\Delta t) \rightarrow f_{CP})} \\ &= A_{CP}^{dir} \cos(\Delta m \Delta t) + A_{CP}^{mix} \sin(\Delta m \Delta t), \end{aligned} \quad (60)$$

where the direct and mixing induced CP-violating asymmetries A_{CP}^{dir} and A_{CP}^{mix} can be written as

$$\mathcal{A}_{CP}^{dir} = \frac{|\lambda_{CP}|^2 - 1}{1 + |\lambda_{CP}|^2}, \quad \mathcal{A}_{CP}^{mix} = \frac{2Im(\lambda_{CP})}{1 + |\lambda_{CP}|^2}, \quad (61)$$

with the CP-violating parameter λ_{CP} is

$$\lambda_{CP} = -\frac{V_{tb}^* V_{td} \langle V \eta^{(\prime)} | H_{eff} | \overline{B}^0 \rangle}{V_{tb} V_{td}^* \langle V \eta^{(\prime)} | H_{eff} | B^0 \rangle}, \quad (62)$$

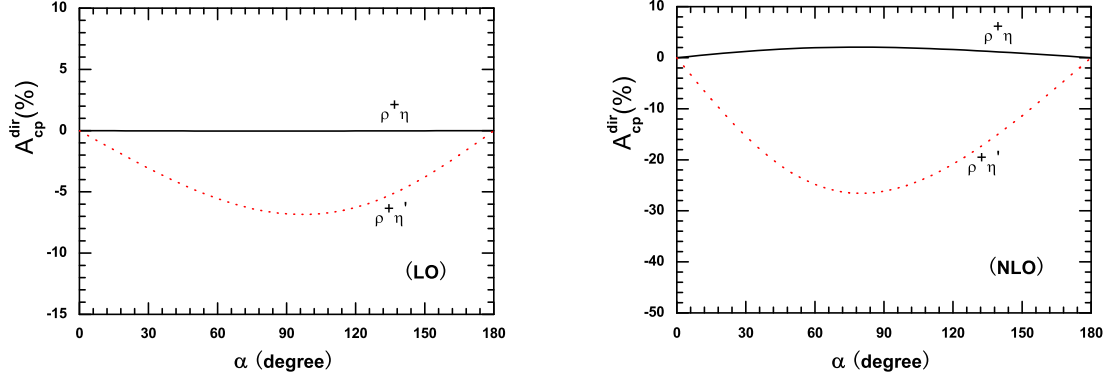


FIG. 8: The α and ω_b -dependence of the CP-violating asymmetries of $B^\pm \rightarrow \rho^\pm \eta^{(\prime)}$ decays for $\alpha = [0^\circ, 180^\circ]$ and $\omega_b = 0.36$ GeV (dotted curve), 0.40 GeV (solid curve) and 0.44 GeV (dashed curve).

TABLE III: The pQCD predictions for the direct, mixing-induced and total CP asymmetries of $B^0 \rightarrow \rho^0(\omega)\eta^{(\prime)}$ decays (in unit of 10^{-2}).

Mode	LO	LO_{NLOWC}	+VC	+QL	+MP	NLO	QCDF
$\mathcal{A}_{CP}^{dir}(B^0 \rightarrow \rho^0 \eta)$	-78.3	-94.4	-91.4	-79.0	-97.4	-89.6	-
$\mathcal{A}_{CP}^{dir}(B^0 \rightarrow \rho^0 \eta')$	77.3	-42.6	-79.8	-96.8	-86.2	-75.7	-
$\mathcal{A}_{CP}^{dir}(B^0 \rightarrow \omega \eta)$	94.6	53.4	45.7	48.7	32.1	33.5	33.4
$\mathcal{A}_{CP}^{dir}(B^0 \rightarrow \omega \eta')$	30.0	26.9	26.5	15.4	-12.1	16.0	-0.2
$\mathcal{A}_{CP}^{mix}(B^0 \rightarrow \rho^0 \eta)$	44.7	26.1	16.9	14.1	17.5	22.7	-
$\mathcal{A}_{CP}^{mix}(B^0 \rightarrow \rho^0 \eta')$	-24.0	-15.9	-46.0	-3.5	-14.4	-49.0	-
$\mathcal{A}_{CP}^{mix}(B^0 \rightarrow \omega \eta)$	-7.4	83.8	40.3	81.5	80.2	39.0	-
$\mathcal{A}_{CP}^{mix}(B^0 \rightarrow \omega \eta')$	58.9	88.7	78.6	82.2	71.6	77.0	-
$\mathcal{A}_{CP}^{tot}(B^0 \rightarrow \rho^0 \eta)$	-24.0	-46.4	-48.9	-42.5	-52.4	-45.0	-
$\mathcal{A}_{CP}^{tot}(B^0 \rightarrow \rho^0 \eta')$	35.5	-34.3	-72.1	-62.2	-60.8	-71.0	-
$\mathcal{A}_{CP}^{tot}(B^0 \rightarrow \omega \eta)$	54.2	73.9	48.1	69.9	58.9	39.8	-
$\mathcal{A}_{CP}^{tot}(B^0 \rightarrow \omega \eta')$	48.4	59.7	54.6	49.4	27.1	47.3	-

If we integrate the time variable t , we will get the total CP asymmetries for $B^0 \rightarrow V \eta^{(\prime)}$ decays,

$$A_{CP} = \frac{1}{1+x^2} A_{CP}^{dir} + \frac{x}{1+x^2} A_{CP}^{mix}, \quad (63)$$

where $x = \Delta m / \Gamma = 0.775$ for the $B^0 - \bar{B}^0$ mixing [22].

The pQCD predictions for the CP-violating asymmetries and the total CP violation

when different NLO contributions are included step by step are listed in Table III. The pQCD predictions with major theoretical errors are given in Eqs. (64-66):

$$\begin{aligned}
\mathcal{A}_{CP}^{dir}(B^0 \rightarrow \rho^0 \eta) &= [-89.6_{-0.9}^{+1.9}(\omega_b)_{-3.9}^{+13.7}(\alpha)_{-0.1}^{+0.7}(a_2)_{-9.0}^{+4.6}(a_{2\rho})] \times 10^{-2}, \\
\mathcal{A}_{CP}^{dir}(B^0 \rightarrow \rho^0 \eta') &= [-75.7_{-4.8}^{+5.6}(\omega_b)_{-7.0}^{+13.1}(\alpha)_{-4.0}^{+6.3}(a_2)_{-9.9}^{+12.9}(a_{2\rho})] \times 10^{-2}, \\
\mathcal{A}_{CP}^{dir}(B^0 \rightarrow \omega \eta) &= [33.5_{-1.4}^{+1.0}(\omega_b)_{-4.6}^{+0.8}(\alpha)_{-6.8}^{+5.9}(a_2)_{-4.4}^{+3.9}(a_{2\omega})] \times 10^{-2}, \\
\mathcal{A}_{CP}^{dir}(B^0 \rightarrow \omega \eta') &= [16.0_{-0.9}^{+0.1}(\omega_b)_{-3.9}^{+3.3}(\alpha)_{-3.2}^{+2.2}(a_2)_{-2.0}^{+1.7}(a_{2\omega})] \times 10^{-2}, \tag{64}
\end{aligned}$$

$$\begin{aligned}
\mathcal{A}_{CP}^{mix}(B^0 \rightarrow \rho^0 \eta) &= [22.7 \pm 6.1(\omega_b)_{-21.8}^{+13.9}(\alpha)_{-12.5}^{+9.6}(a_2)_{-26.5}^{+23.6}(a_{2\rho})] \times 10^{-2}, \\
\mathcal{A}_{CP}^{mix}(B^0 \rightarrow \rho^0 \eta') &= [-49.0_{-0.8}^{+1.9}(\omega_b)_{-8.1}^{+16.0}(\alpha)_{-4.2}^{+1.8}(a_2)_{-17.8}^{+18.6}(a_{2\rho})] \times 10^{-2}, \\
\mathcal{A}_{CP}^{mix}(B^0 \rightarrow \omega \eta) &= [39.0_{-0.2}^{+0.3}(\omega_b)_{-66.2}^{+50.6}(\alpha)_{-3.3}^{+5.9}(a_2)_{-1.9}^{+2.9}(a_{2\omega})] \times 10^{-2}, \\
\mathcal{A}_{CP}^{mix}(B^0 \rightarrow \omega \eta') &= [77.0_{-0.1}^{+0.4}(\omega_b)_{-52.9}^{+22.0}(\alpha)_{-0.1}^{+0.9}(a_2)_{-0.0}^{+0.3}(a_{2\omega})] \times 10^{-2}, \tag{65}
\end{aligned}$$

$$\begin{aligned}
\mathcal{A}_{CP}^{tot}(B^0 \rightarrow \rho^0 \eta) &= [-45.0_{-1.7}^{+2.4}(\omega_b)_{-13.0}^{+15.3}(\alpha)_{-6.1}^{+5.1}(a_2)_{-15.7}^{+17.1}(a_{2\rho})] \times 10^{-2}, \\
\mathcal{A}_{CP}^{tot}(B^0 \rightarrow \rho^0 \eta') &= [-71.0_{-2.1}^{+2.9}(\omega_b)_{-0.0}^{+4.2}(\alpha)_{-1.7}^{+1.9}(a_2)_{-0.6}^{+2.8}(a_{2\rho})] \times 10^{-2}, \\
\mathcal{A}_{CP}^{tot}(B^0 \rightarrow \omega \eta) &= [39.8_{+0.6}^{-0.7}(\omega_b)_{-31.5}^{+20.2}(\alpha)_{-5.8}^{+6.6}(a_2)_{-3.6}^{+3.9}(a_{2\omega})] \times 10^{-2}, \\
\mathcal{A}_{CP}^{tot}(B^0 \rightarrow \omega \eta') &= [47.3_{-0.6}^{+0.2}(\omega_b)_{-23.6}^{+8.2}(\alpha)_{-2.1}^{+1.8}(a_2) \pm 1.2(a_{2\omega})] \times 10^{-2}, \tag{66}
\end{aligned}$$

where the dominant errors come from the variations of $\omega_b = 0.4 \pm 0.04$ GeV, $\alpha = 100^\circ \pm 20^\circ$, and Gegenbauer coefficient $a_2 = 0.115 \pm 0.115$, $a_{2\rho} = a_{2\omega} = 0.15 \pm 0.15$.

For the CP-violating asymmetries of $B^0 \rightarrow \rho^0(\omega)\eta^{(\prime)}$ decays, unfortunately, there is no data available currently. For $B^0 \rightarrow \phi\eta^{(\prime)}$ decays, there is no CP violation. The reasons are simple: (a) the total decay amplitude at the LO level as given in Eq. (11) is proportional to only one CKM factor ξ_t ; and (b) among the NLO contributions considered here, only the vertex correction (real correction) is relevant for this decay mode.

VI. SUMMARY

In this paper, we calculate some NLO contributions to the branching ratios and CP-violating asymmetries of $B^\pm \rightarrow \rho^\pm \eta^{(\prime)}$ and $B^0 \rightarrow \rho^0(\omega, \phi)\eta^{(\prime)}$ decays by employing the pQCD factorization approach.

From our calculations and phenomenological analysis, we found the following results:

- The pQCD predictions for the form factors of $B \rightarrow \rho, \omega$ and $\eta^{(\prime)}$ transitions are $A_0^{B \rightarrow \rho}(0) = 0.32_{-0.04}^{+0.05}(\omega_b)$, $A_0^{B \rightarrow \omega}(0) = 0.29_{-0.03}^{+0.04}(\omega_b)$ and $F_0^{B \rightarrow \eta^{(\prime)}}(0) = 0.22 \pm 0.03(\omega_b)$ for $\omega_b = 0.40 \pm 0.04$ GeV, which agree very well with those obtained in QCD sum rule calculations.
- For $B^\pm \rightarrow \rho^\pm \eta$ decay, the inclusion of partial NLO contributions can improve the agreement between the pQCD predictions and the measured values. For the neutral decays, the NLO contributions can provide significant enhancements to the LO

predictions:

$$\begin{aligned}
Br(B^\pm \rightarrow \rho^\pm \eta) &= [6.7_{-1.9}^{+2.6}] \times 10^{-6}, \\
Br(B^\pm \rightarrow \rho^\pm \eta') &= [4.6_{-1.4}^{+1.6}] \times 10^{-6}, \\
Br(B^0 \rightarrow \rho^0 \eta) &= [1.3_{-0.6}^{+1.3}] \times 10^{-7}, \\
Br(B^0 \rightarrow \rho^0 \eta') &= [1.0 \pm 0.5] \times 10^{-7}, \\
Br(B^0 \rightarrow \omega \eta) &= [7.1_{-2.8}^{+3.7}] \times 10^{-7}, \\
Br(B^0 \rightarrow \omega \eta') &= [5.5_{-2.6}^{+3.1}] \times 10^{-7}, \\
Br(B^0 \rightarrow \phi \eta) &= [1.1_{-0.9}^{+6.2}] \times 10^{-8}, \\
Br(B^0 \rightarrow \phi \eta') &= [1.7_{-1.0}^{+16.1}] \times 10^{-8},
\end{aligned} \tag{67}$$

where the various errors as given in Eq. (56) have been added in quadrature.

- The pQCD predictions for $\mathcal{A}_{CP}^{dir}(B^\pm \rightarrow \rho^\pm \eta^{(\prime)})$ are consistent with the data, but both the theoretical and experimental errors are still large. For other neutral decays, the pQCD predictions for CP violating asymmetries are generally large in magnitude and could be tested by the forthcoming LHCb experiments.
- Only the NLO contributions from vertex correction, quark-loops and chromo-magnetic penguins are calculated here. The NLO corrections from the hard-spectator and annihilations diagrams are still absent now. It is an urgent task to do the relevant calculations, in order to provide a complete NLO calculation in the pQCD approach.

Acknowledgments

The authors are very grateful to Kavli Institute for Theoretical Physics China, Beijing, China, where part of this work was done. This work is partly supported by the National Natural Science Foundation of China under Grant No.10575052 and 10735080.

APPENDIX A: WAVE FUNCTIONS AND INPUT PARAMETERS

The B meson is treated as a heavy-light system. For the B meson wave function, since the contribution of $\bar{\phi}_B$ is numerically small [24], we here only consider the contribution of Lorentz structure

$$\Phi_B = \frac{1}{\sqrt{2N_c}} (\not{P}_B + m_B) \gamma_5 \phi_B(\mathbf{k}_1), \tag{A1}$$

with

$$\phi_B(x, b) = N_B x^2 (1-x)^2 \exp \left[-\frac{M_B^2 x^2}{2\omega_b^2} - \frac{1}{2}(\omega_b b)^2 \right], \tag{A2}$$

where ω_b is a free parameter and we take $\omega_b = 0.4 \pm 0.04$ GeV in numerical calculations, and $N_B = 101.445$ is the normalization factor for $\omega_b = 0.4$.

For the considered decays, the vector meson V is longitudinally polarized. The longitudinal polarized component of the wave function is defined as:

$$\phi_V = \frac{1}{\sqrt{2N_c}} \left\{ \not{\epsilon} \left[m_V \phi_V(x) + \not{p}_V \phi_V^t(x) \right] + m_V \phi_V^s(x) \right\}, \quad (\text{A3})$$

where the first term is the leading twist (twist-2) wave function, while the second and third terms are twist-3 wave functions.

The twist-2 DA's for longitudinally polarized vector meson can be parameterized as:

$$\phi_V(x) = \frac{f_V}{2\sqrt{2N_c}} 6x(1-x) \left[1 + a_{2V} C_2^{3/2}(2x-1) \right], \quad (\text{A4})$$

for $V = \rho, \omega, \phi$; and f_V is the decay constant of the vector meson with longitudinal polarization, and numerically [25]:

$$f_\rho = 216 \text{ MeV}, \quad f_\omega = 187 \text{ MeV}, \quad f_\phi = 215 \text{ MeV}. \quad (\text{A5})$$

The Gegenbauer coefficients have been studied extensively in the literature. Here we adopt the following values from the recent updates [25]:

$$a_{2\rho} = a_{2\omega} = 0.15 \pm 0.15, \quad a_{2\phi} = 0.2 \pm 0.2. \quad (\text{A6})$$

We shall vary the Gegenbauer coefficients of the twist-2 distribution amplitudes by 100%, which is larger than the error specified in [25]. Therefore, the theoretical uncertainty of our predictions from this source is conservative.

As for the twist-3 DAs ϕ_V^s and ϕ_V^t , we adopt their asymptotic form [26]:

$$\phi_V^s(x) = \frac{3f_V^T}{2\sqrt{2N_c}}(1-2x), \quad \phi_V^t(x) = \frac{3f_V^T}{2\sqrt{2N_c}}(2x-1)^2, \quad (\text{A7})$$

For $\eta^{(\prime)}$ meson, the wave function for $q\bar{q}$ ($q = u, d$) components of $\eta^{(\prime)}$ meson are given as

$$\Phi_{\eta_q}(P, x, \zeta) \equiv \frac{1}{\sqrt{2N_C}} \gamma_5 \left[\not{P} \phi_{\eta_q}^A(x) + m_0^{\eta_q} \phi_{\eta_q}^P(x) + \zeta m_0^{\eta_q} (\not{p}\not{\eta} - v \cdot n) \phi_{\eta_q}^T(x) \right], \quad (\text{A8})$$

where P and x are the momentum and the momentum fraction of η_q , respectively. We assumed here that the wave function of η_q is same as the π wave function. The parameter ζ is either +1 or -1 depending on the assignment of the momentum fraction x . The $s\bar{s}$ component of the wave function can be similarly defined.

For the mixing of $\eta - \eta'$ system, we here use the quark-flavor basis, that is the $\eta_q = (u\bar{u} + d\bar{d})/\sqrt{2}$ and $\eta_s = s\bar{s}$. Then the physical states η and η' are related to the flavor states through a single mixing angle ϕ ,

$$\begin{pmatrix} \eta \\ \eta' \end{pmatrix} = \begin{pmatrix} \cos \phi & -\sin \phi \\ \sin \phi & \cos \phi \end{pmatrix} \begin{pmatrix} \eta_q \\ \eta_s \end{pmatrix}, \quad (\text{A9})$$

The relation between the decay constants $(f_\eta^q, f_\eta^s, f_{\eta'}^q, f_{\eta'}^s)$ and (f_q, f_s) can be written as

$$\begin{aligned} f_\eta^q &= f_q \cos \phi, & f_\eta^s &= -f_s \sin \phi, \\ f_{\eta'}^q &= f_q \sin \phi, & f_{\eta'}^s &= f_s \cos \phi. \end{aligned} \quad (\text{A10})$$

The chiral enhancement m_0^q and m_0^s associated with the two-parton twist-3 η_q and η_s meson distribution amplitudes have been defined as [15]

$$m_0^q = \frac{m_{qq}^2}{2m_q} = \frac{1}{2m_q} [m_\eta^2 \cos^2 \phi + m_{\eta'}^2 \sin^2 \phi - \frac{\sqrt{2}f_s}{f_q} (m_{\eta'}^2 - m_\eta^2) \cos \phi \sin \phi], \quad (\text{A11})$$

$$m_0^s = \frac{m_{ss}^2}{2m_s} = \frac{1}{2m_s} [m_{\eta'}^2 \cos^2 \phi + m_\eta^2 \sin^2 \phi - \frac{\sqrt{2}f_q}{f_s} (m_{\eta'}^2 - m_\eta^2) \cos \phi \sin \phi], \quad (\text{A12})$$

by assuming the exact isospin symmetry $m_q = m_u = m_d$. The three input parameters f_q , f_s and ϕ have been extracted from the data of the relevant exclusive processes[27]:

$$f_q = (1.07 \pm 0.02)f_\pi, \quad f_s = (1.34 \pm 0.06)f_\pi, \quad \phi = 39.3^\circ \pm 1.0^\circ, \quad (\text{A13})$$

It is still unclear for the possible gluonic component of η' meson. From currently known studies[10, 11, 12] we believe that there is no large room left for the contribution due to the gluonic component of η' , and therefore will neglect the possible gluonic component in η' meson.

The distribution amplitude $\phi_{\eta_q}^{A,P,T}$ represents the axial vector, pseudoscalar and tensor component of the wave function respectively [29]. They are given as:

$$\phi_{\eta_q}^A(x) = \frac{f_{\eta_q}}{2\sqrt{2}N_c} 6x(1-x) \left[1 + a_1^{\eta_q} C_1^{3/2}(2x-1) + a_2^{\eta_q} C_2^{3/2}(2x-1) + a_4^{\eta_q} C_4^{3/2}(2x-1) \right], \quad (\text{A14})$$

$$\phi_{\eta_q}^P(x) = \frac{f_{\eta_q}}{2\sqrt{2}N_c} \left[1 + (30\eta_3 - \frac{5}{2}\rho_{\eta_q}^2) C_2^{1/2}(2x-1) - 3 \left\{ \eta_3\omega_3 + \frac{9}{20}\rho_{\eta_q}^2(1 + 6a_2^{\eta_q}) \right\} C_4^{1/2}(2x-1) \right], \quad (\text{A15})$$

$$\phi_{\eta_q}^T(x) = \frac{f_{\eta_q}}{2\sqrt{2}N_c} (1-2x) \left[1 + 6 \left(5\eta_3 - \frac{1}{2}\eta_3\omega_3 - \frac{7}{20}\rho_{\eta_q}^2 - \frac{3}{5}\rho_{\eta_q}^2 a_2^{\eta_q} \right) \cdot (1-10x+10x^2) \right], \quad (\text{A16})$$

with

$$\rho_{\eta_q} = 2m_q/m_{qq}, \quad a_1^{\eta_{q\bar{q}}} = 0, \quad a_2^{\eta_{q\bar{q}}} = 0.115 \pm 0.115, \quad a_4^{\eta_{q\bar{q}}} = -0.015. \quad (\text{A17})$$

and the Gegenbauer polynomials $C_n^\nu(t)$,

$$C_2^{1/2}(t) = \frac{1}{2}(3t^2 - 1), \quad C_4^{1/2}(t) = \frac{1}{8}(3 - 30t^2 + 35t^4), \quad (\text{A18})$$

$$C_1^{3/2}(t) = 3t, \quad C_2^{3/2}(t) = \frac{3}{2}(5t^2 - 1), \quad (\text{A19})$$

$$C_4^{3/2}(t) = \frac{15}{8}(1 - 14t^2 + 21t^4). \quad (\text{A20})$$

The Gegenbauer coefficients can vary by 100%, but we do not consider the uncertainty from the coefficients $a_4^{\eta_{q\bar{q}}}$, to which our predictions are insensitive. The values of other parameters are $\eta_3 = 0.015$ and $\omega = -3.0$.

As to the wave function of the $s\bar{s}$ components, we also use the same form as $q\bar{q}$ but with some parameters changed :

$$\rho_{\eta_s} = 2m_s/m_{ss}, \quad a_1^{\eta_s} = 0, \quad a_2^{\eta_s} = 0.115 \pm 0.115, \quad a_4^{\eta_s} = -0.015. \quad (\text{A21})$$

Besides those specified in the text, the following input parameters will also be used in the numerical calculations:

$$\begin{aligned} f_\pi &= 130\text{MeV}, & f_B &= 210\text{MeV}, & m_\eta &= 547.5\text{MeV}, & m_{\eta'} &= 957.8\text{MeV}, \\ m_q &= 5.6\text{MeV}, & m_s &= 130 \pm 30\text{MeV}, & m_B &= 5.28\text{GeV}, \\ m_\rho &= 774\text{MeV}, & m_\omega &= 780\text{MeV} & m_\phi &= 1.02\text{GeV}, & m_W &= 80.41\text{GeV}, \\ \tau_{B^0} &= 1.528\text{ps}, & \tau_{B^+} &= 1.643\text{ps}, \end{aligned} \quad (\text{A22})$$

For the CKM quark-mixing matrix, we use the Wolfenstein parametrization as given in Ref.[22, 23].

$$\begin{aligned} V_{ud} &= 0.9745, & V_{us} &= \lambda = 0.2200, & |V_{ub}| &= 4.31 \times 10^{-3}, \\ V_{cd} &= -0.224, & V_{cb} &= 0.0413, \\ |V_{td}| &= 7.4 \times 10^{-3}, & V_{ts} &= -0.042, & |V_{tb}| &= 0.9991, \end{aligned} \quad (\text{A23})$$

with the CKM angles $\beta = 21.6^\circ$, $\gamma = 60^\circ \pm 20^\circ$ and $\alpha = 100^\circ \pm 20^\circ$.

APPENDIX B: RELATED FUNCTIONS

We show here the function h_i 's, coming from the Fourier transformations of $H^{(0)}$,

$$\begin{aligned} h_e(x_1, x_2, b_1, b_2) &= K_0(\sqrt{x_1 x_2} m_B b_1) [\theta(b_1 - b_2) K_0(\sqrt{x_2} m_B b_1) I_0(\sqrt{x_2} m_B b_2) \\ &\quad + \theta(b_2 - b_1) K_0(\sqrt{x_2} m_B b_2) I_0(\sqrt{x_2} m_B b_1)] S_t(x_2), \end{aligned} \quad (\text{B1})$$

$$\begin{aligned} h_a(x_2, x_3, b_2, b_3) &= K_0\left(i\sqrt{(1-x_2)x_3} m_B b_2\right) [\theta(b_3 - b_2) K_0(i\sqrt{x_3} m_B b_3) I_0(i\sqrt{x_3} m_B b_2) \\ &\quad + \theta(b_2 - b_3) K_0(i\sqrt{x_3} m_B b_2) I_0(i\sqrt{x_3} m_B b_3)] S_t(x_3), \end{aligned} \quad (\text{B2})$$

$$\begin{aligned} h_n(x_1, x_2, x_3, b_1, b_3) &= \left\{ \theta(b_1 - b_3) K_0(M_B \sqrt{x_1 x_2} b_1) I_0(M_B \sqrt{x_1 x_2} b_3) \right. \\ &\quad \left. + \theta(b_3 - b_1) K_0(M_B \sqrt{x_1 x_2} b_3) I_0(M_B \sqrt{x_1 x_2} b_1) \right\} \\ &\quad \cdot \left(\begin{array}{l} \frac{\pi i}{2} H_0(\sqrt{(x_2(x_3 - x_1))} M_B b_3), \text{ for } x_1 - x_3 < 0 \\ K_0^{(1)}(\sqrt{(x_2(x_1 - x_3))} M_B b_3), \text{ for } x_1 - x_3 > 0 \end{array} \right), \end{aligned} \quad (\text{B3})$$

$$\begin{aligned} h_{na}(x_1, x_2, x_3, b_1, b_3) &= \left\{ \theta(b_1 - b_3) K_0(i\sqrt{(1-x_2)x_3} b_1 M_B) I_0(i\sqrt{(1-x_2)x_3} b_3 M_B) \right. \\ &\quad \left. + (\theta(b_3 - b_1) K_0(i\sqrt{(1-x_2)x_3} b_3 M_B) I_0(i\sqrt{(1-x_2)x_3} b_1 M_B)) \right\} \\ &\quad \cdot \left(\begin{array}{l} K_0(M_B \sqrt{(x_1 - x_3)(1-x_2)} b_1), \text{ for } x_1 - x_3 > 0 \\ \frac{\pi i}{2} H_0^{(1)}(M_B \sqrt{(x_3 - x_1)(1-x_2)} b_1), \text{ for } x_1 - x_3 < 0 \end{array} \right), \end{aligned} \quad (\text{B4})$$

$$\begin{aligned}
h'_{na}(x_1, x_2, x_3, b_1, b_2) = & \left\{ \theta(b_1 - b_3) K_0(i\sqrt{(1-x_2)x_3}b_1 M_B) I_0(i\sqrt{(1-x_2)x_3}b_3 M_B) \right. \\
& + \left. \theta(b_3 - b_1) K_0(i\sqrt{(1-x_2)x_3}b_3 M_B) I_0(i\sqrt{(1-x_2)x_3}b_1 M_B) \right\} \\
& \cdot \left(\begin{array}{ll} K_0(M_B F_1 b_1), & \text{for } F_1^2 > 0 \\ \frac{\pi i}{2} H_0^{(1)}(M_B \sqrt{|F_1^2|} b_1), & \text{for } F_1^2 < 0 \end{array} \right), \quad (\text{B5})
\end{aligned}$$

where J_0 is the Bessel function and K_0, I_0 are modified Bessel functions $K_0(-ix) = -(\pi/2)Y_0(x) + i(\pi/2)J_0(x)$, and $F_{(1)}$'s are defined by

$$F_{(1)}^2 = 1 - x_2(1 - x_3 - x_1). \quad (\text{B6})$$

The threshold resummation form factor $S_t(x_i)$ is adopted from Ref .[28].It has been parametrized as

$$S_t(x) = \frac{2^{1+2c}\Gamma(3/2+c)}{\sqrt{\pi}\Gamma(1+c)} [x(1-x)]^c, \quad (\text{B7})$$

where the parameter $c = 0.3$. This function is normalized to unity. The evolution factors $E_e^{(t)}$ and $E_a^{(t)}$ are given by

$$\begin{aligned}
E_e(t) &= \alpha_s(t) \exp[-S_{ab}(t)], \\
E'_e(t) &= \alpha_s(t) \exp[-S_{cd}(t)]|_{b_2=b_1}, \\
E_a(t) &= \alpha_s(t) \exp[-S_{gh}(t)], \\
E'_a(t) &= \alpha_s(t) \exp[-S_{ef}(t)]|_{b_2=b_3}, \quad (\text{B8})
\end{aligned}$$

The Sudakov factors used in the text are defined as

$$\begin{aligned}
S_{ab}(t) &= s \left(x_1 m_B / \sqrt{2}, b_1 \right) + s \left(x_2 m_B / \sqrt{2}, b_2 \right) + s \left((1-x_2) m_B / \sqrt{2}, b_2 \right) \\
&\quad - \frac{1}{\beta_1} \left[\ln \frac{\ln(t/\Lambda)}{-\ln(b_1 \Lambda)} + \ln \frac{\ln(t/\Lambda)}{-\ln(b_2 \Lambda)} \right], \quad (\text{B9})
\end{aligned}$$

$$\begin{aligned}
S_{cd}(t) &= s \left(x_1 m_B / \sqrt{2}, b_1 \right) + s \left(x_2 m_B / \sqrt{2}, b_1 \right) + s \left((1-x_2) m_B / \sqrt{2}, b_1 \right) \\
&\quad + s \left(x_3 m_B / \sqrt{2}, b_3 \right) + s \left((1-x_3) m_B / \sqrt{2}, b_3 \right) \\
&\quad - \frac{1}{\beta_1} \left[2 \ln \frac{\ln(t/\Lambda)}{-\ln(b_1 \Lambda)} + \ln \frac{\ln(t/\Lambda)}{-\ln(b_3 \Lambda)} \right], \quad (\text{B10})
\end{aligned}$$

$$\begin{aligned}
S_{ef}(t) &= s \left(x_1 m_B / \sqrt{2}, b_1 \right) + s \left(x_2 m_B / \sqrt{2}, b_2 \right) + s \left((1-x_2) m_B / \sqrt{2}, b_2 \right) \\
&\quad + s \left(x_3 m_B / \sqrt{2}, b_2 \right) + s \left((1-x_3) m_B / \sqrt{2}, b_2 \right) \\
&\quad - \frac{1}{\beta_1} \left[\ln \frac{\ln(t/\Lambda)}{-\ln(b_1 \Lambda)} + 2 \ln \frac{\ln(t/\Lambda)}{-\ln(b_2 \Lambda)} \right], \quad (\text{B11})
\end{aligned}$$

$$\begin{aligned}
S_{gh}(t) &= s \left(x_2 m_B / \sqrt{2}, b_2 \right) + s \left(x_3 m_B / \sqrt{2}, b_3 \right) + s \left((1-x_2) m_B / \sqrt{2}, b_2 \right) \\
&\quad + s \left((1-x_3) m_B / \sqrt{2}, b_3 \right) - \frac{1}{\beta_1} \left[\ln \frac{\ln(t/\Lambda)}{-\ln(b_1 \Lambda)} + \ln \frac{\ln(t/\Lambda)}{-\ln(b_2 \Lambda)} \right], \quad (\text{B12})
\end{aligned}$$

where the function $s(q, b)$ are defined in the Appendix A of Ref.[7]. The scale t_i 's in the above equations are chosen as

$$\begin{aligned}
t_a &= \max(\sqrt{x_2}m_B, \sqrt{x_1x_2}m_B, 1/b_1, 1/b_2) , \\
t'_a &= \max(\sqrt{x_1}m_B, \sqrt{x_1x_2}m_B, 1/b_1, 1/b_2) , \\
t_b &= \max(\sqrt{x_2|1-x_3-x_1|}m_B, \sqrt{x_1x_2}m_B, 1/b_1, 1/b_3) , \\
t'_b &= \max(\sqrt{x_2|x_3-x_1|}m_B, \sqrt{x_1x_2}m_B, 1/b_1, 1/b_3) , \\
t_c &= \max(\sqrt{(1-x_2)x_3}m_B, \sqrt{|x_1-x_3|(1-x_2)}m_B, 1/b_1, 1/b_3) , \\
t'_c &= \max(\sqrt{|1-x_2(1-x_3-x_1)|}m_B, \sqrt{(1-x_2)x_3}m_B, 1/b_1, 1/b_3) , \\
t_d &= \max(\sqrt{(1-x_2)x_3}m_B, \sqrt{(1-x_2)}m_B, 1/b_2, 1/b_3) , \\
t'_d &= \max(\sqrt{(1-x_2)x_3}m_B, \sqrt{x_3}m_B, 1/b_2, 1/b_3) .
\end{aligned} \tag{B13}$$

-
- [1] I.I. Bigi and A.I. Sanda, *CP Violation* (Cambridge University Press, Cambridge, England, 2000); G.C. Branco, L. Lavoura and J.P. Silva, *CP Violation* (Oxford University Press, Oxford, England, 1999); R. Fleischer, Phys. Rep. **370** (2002) 537; T. Hurth, Rev. Mod. Phys. **75** (2003) 1159.
- [2] H.-n. Li, Prog. Part. & Nucl. Phys. **51**, 85 (2003) and references therein.
- [3] M. Beneke, G. Buchalla, M. Neubert, and C.T. Sachrajda, Phys. Rev. Lett. **83**, 1914 (1999); Nucl. Phys. B **591**, 313 (2000).
- [4] C.W.Bauer, D.Pirjol, I.Z. Rothstein and I.W. Stewart, Phys. Rev. D **70**, 054015 (2004); M. Beneke and T. Feldmann, Nucl. Phys. B **685**, 249(2004).
- [5] D.S. Du, H.J. Gong, J.F. Sun, D.S. Yang, and G.H. Zhu, Phys. Rev. D **65**, 074001(2002) *ibid* **65**,094025 (2002); J.F. Sun, G.H. Zhu and D.S. Du, Phys. Rev. D **68**, 054003 (2003).
- [6] Y.-Y. Keum, H.-n. Li and A.I. Sanda, Phys. Rev. D **63**, 054008 (2001).
- [7] C.D. Lü, K. Ukai and M.Z. Yang, Phys. Rev. D **63**, 074009 (2001).
- [8] H.-n. Li, Phys. Rev. D **64**, 014019 (2001); C.-H. Chen, Y.-Y. Keum, and H.-n. Li, Phys. Rev. D **64**,112002 (2001); Phys. Rev. D **66**,054013 (2002); Y.-Y. Keum and A.I. Sanda, Phys. Rev. D **67**, 054009 (2003).
- [9] Y. Li, C.D. Lü, Z.J. Xiao, and X.Q. Yu, Phys. Rev. D **70**, 034009 (2004); Y. Li, C.D. Lü, and Z.J. Xiao, J. Phys. G **31**, 273 (2005).
- [10] X. Liu, H.S. Wang, Z.J. Xiao, L.B. Guo, and C.D. Lü, Phys. Rev. D **73**, 074002 (2006);
- [11] D.Q. Guo, X.F. Chen, and Z.J. Xiao, Phys. Rev. D **75**, 054033 (2007).
- [12] L.B. Guo, Q.G. Xu and Z.J. Xiao, Phys. Rev. D **75**, 014019 (2007).
- [13] A. Ali, G. Kramer, Y. Li, C.D. Lü, Y.L. Shen, W. Wang and Y.M. Wang, Phys. Rev. D **76**, 074018 (2007).
- [14] Z.J. Xiao, X.F. Chen and D.Q. Guo, Eur. Phys. J. C **50**, 363 (2007); Z.J. Xiao, X. Liu and H.S. Wang, Phys. Rev. D **75**, 034017 (2007).
- [15] H.-n. Li, S. Mishima, A.I. Sanda, Phys. Rev. D **72**, 114005 (2005).
- [16] H.-n. Li, S. Mishima, Phys. Rev. D **74**, 094020 (2006).
- [17] H.-n. Li, Phys. Rev. D **66**, 094010 (2002).

- [18] G. Buchalla, A.J. Buras, and M.E. Lautenbacher, *Rev. Mod. Phys.* **68**, 1125 (1996).
- [19] M. Beneke and M. Neubert, *Nucl. Phys. B* **675**, 333 (2003).
- [20] M. Bander, D. Silverman and A. Soni, *Phys. Rev. Lett.* **43**, 242 (1979); J.M. Gerard and W.S. Hou, *Phys. Rev. D* **43**, 2909 (1991);
- [21] S. Mishima and A.I. Sanda, *Prog. Theor. Phys.* **110**, 549 (2003).
- [22] Particle Data Group, W.-M. Yao *et al.*, *J. Phys. G* **33**, 1 (2006).
- [23] E. Barberio *et al.*, (Heavy Flavor Averaging Group), hep-ex/0704.3575; for update see: <http://www.slac.stanford.edu/xorg/hfag>.
- [24] C.D. Lü, M.Z. Yang, *Eur. Phys. J. C* **28**, 515 (2003).
- [25] P. Ball, G.W. Jones and R. Zwicky, *Phys. Rev. D* **75**, 054004 (2007).
- [26] H.-n. Li, *Phys. Lett. B* **622**, 63 (2005).
- [27] T. Feldmann, P. Kroll, and B. Stech, *Phys. Rev. D* **58**, 114006 (1998); *Phys. Lett. B* **449**, 339 (1999).
- [28] T. Kurimoto, H.N. Li, A.I. Sanda, *Phys. Rev. D* **65**, 014007 (2001).
- [29] P. Ball, V.M. Braun, Y. Koike, and K. Tanaka, *Nucl. Phys. B* **529**, 323 (1998); P. Ball, *J. High Energy Phys.* 09 (1998) 005; P. Ball and R. Zwicky, *Phys. Rev. D* **71**, 014015 (2005); *J. High Energy Phys.* 04 (2006) 046.